Geologic Map of the Bonners Ferry 30 x 60 Minute Quadrangle, Idaho and Montana

Mapped and Compiled by
Roy M. Breckenridge, Russell F. Burmester,
Reed S. Lewis, and Mark D. McFaddan

2014

Geologic Map of the Bonners Ferry 30 x 60 Minute Quadrangle, Idaho and Montana

Mapped and Compiled by
Roy M. Breckenridge, Russell F. Burmester,
Reed S. Lewis, and Mark D. McFadden

INTRODUCTION

Geology depicted here is the result of field work from 2008 to 2012 and compilation of previous mapping. The area covered by each source is shown on Figure 2. Quaternary deposits were mapped by R.M. Breckenridge over several field seasons through 2012. Bedrock geology is based partly on unpublished 7.5 minute mapping by F.K. Miller and R.F. Burmester from the 1980s, as well as local mapping by others. Bedrock was also remapped during field work in 2008-2012 to apply unit definitions and contact placements consistent with current mapping to the south. This redefinition included subdivision of the Prichard Formation based on mapping by Cominco geologists (Michael Zientek, written commun., 2003) and revision of the middle Belt carbonate, or Wallace Formation. See Harrison and Jobin (1963) for the history of naming Belt-Purcell Supergroup units to the south; departures from their naming scheme are explained within descriptions of affected units. Overall, the bedrock areas of the eastern part of the map differ little from Miller and Burmester (2004); the chief differences are in the Prichard Formation subdivision and structures.

Low metamorphic grade metasedimentary rocks of the Mesoproterozoic Belt-Purcell Supergroup underlie most of the area. Higher metamorphic grade rocks of the Priest River complex in the western part of the map appear to have protoliths of the same age; this relationship and their lithologies are consistent with their derivation from lower Prichard strata. Some igneous rocks are coeval with deposition of the Belt-Purcell Supergroup, but most granitoids are Cretaceous in age, and most hypabyssal rocks are constrained to the Eocene.

The Purcell Trench is a major structural and physiographic feature that extends south from Canada over 130 km (80 mi) into the Idaho Panhandle. It is bounded on the east by the Purcell and Cabinet Mountains and on the west by the Selkirk Mountains. The present landscape is largely a result of glaciation during the late Pleistocene. Quaternary deposits from glaciers and their damming and diversion of rivers cover much of the highlands and valleys.

DESCRIPTION OF MAP UNITS

Intrusive rocks are classified according to International Union of Geological Sciences nomenclature using normalized values of modal quartz (Q), alkali feldspar (A) and plagioclase (P) on a ternary diagram (Streckeisen, 1976). Mineral modifiers are listed in order of increasing abundance for igneous rocks. Grain size classification of unconsolidated and consolidated sediment is based on the Wentworth scale (Lane, 1947). Bedding thicknesses and lamination type are after McKee and Weir (1963), and Winston (1986). Grain sizes and bedding thicknesses are given in abbreviation of metric units (e.g., dm=decimeter). Unit thicknesses, distances and elevations are listed in both metric and English units. Multiple lithologies within a rock unit description are listed in order of decreasing abundance, and stratigraphic units are described from bottom to top where possible. Soil descriptions for Quaternary units are after Chugg and Fosberg (1980) and Weisel (2005). Interpretations of kinematic indicators are based on Simpson and Schmid (1983) for ductile fabrics, and Petit (1987) and Doblas (1998) for brittle fabrics. Magnetic susceptibilities for some units are in Table 1.

QUATERNARY DEPOSITS

MAN-MADE DEPOSITS

m—Man-made land (historical)—Highway fills along US 95 and bridges, railroad rights of way and trestles, and dams. Numerous small fills in and around Bonners Ferry are not mapped.

ALLUVIAL AND LACUSTRINE DEPOSITS

Qar—Active river wash (Holocene)—Silt, clay, and sand deposits in the active channel and floodplain confined by levees of the Kootenai River, and some along the Moyie River. Most channel substrates are modern deposits related to the 1972 closure of Libby Dam in Montana about 100 km (62 mi) upstream of Bonners Ferry (Barton, 2003; Barton and others, 2004).

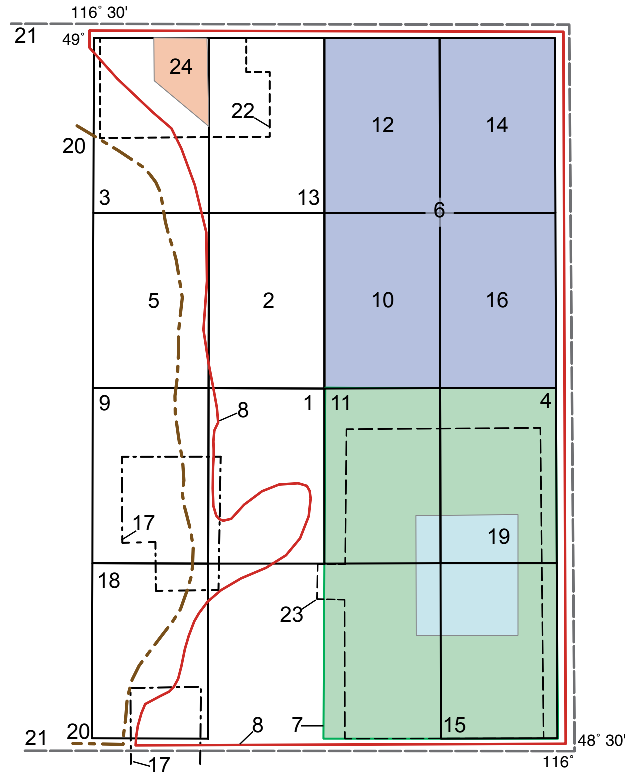

1. Breckenridge and others, 2009
2. Breckenridge and others, 2010
3. Breckenridge and others, 2011
4. Breckenridge and others, 2012
5. Breckenridge and others, 2013
6. Burmester, 1985
7. Burmester, 1986
8. Burmester, R.F., unpublished mapping 1982-1986
9. Burmester and others, 2009
10. Burmester and others, 2010a
11. Burmester and others, 2010b
12. Burmester and others, 2011a
13. Burmester and others, 2011b
14. Burmester and others, 2012a
15. Burmester and others, 2012b
16. Burmester and others, 2012c
17. Doughty, 1995
18. McFaddan and others, 2009
19. Miller, 1973
20. Miller, F.K., unpublished mapping, 1979, 1981, 1991, 1993, 1994.
21. Miller and Burmester, 2004
22. Newton and others, 1960
23. Redfield, 1986
24. Staatz, 1972

Figure 2. *Index of geologic mapping used as sources of data.*

Qal—Alluvium (Holocene)—Alluvial deposits of the Kootenai River and its tributary streams. Unstratified to stratified, moderately- to well-sorted silt, sand, and locally-derived pebble and cobble gravels. Mostly reworked glacial deposits in the Purcell Trench and post-glacial colluvium in the surrounding mountains. Schnoorson-Ritz-Farnhampton soils association; typical soils are very deep silty clay loams, silt loams, and mucky silt loams in basins, swales, and meander scars on low terraces, flood plains, and natural levees. Thickness ranges from three to more than 10 m (10 to >33 ft).

Intrusive Rocks

Unit	Sample number	Latitude	Longitude	7.5′ quadrangle	Instrument	Kbulk
Tl	86RED107	48.5466	-116.1978	Leonia	KLY-3S	2.13E-02
Tl	86BT08	48.7083	-116.3500	BonnersFerry	KLY-3S	1.86E-02
Kgbf	2B78	48.7080	-116.3422	Bonners Ferry	KLY-3S	9.48E-03
Kgbf	86BT09	48.7083	-116.3500	BonnersFerry	KLY-3S	7.80E-03
Kgbf	08RB015	48.6930	-116.3312	Bonners Ferry	KLY-3S	5.87E-03
Kgbf	08RB015	48.6930	-116.3312	Bonners Ferry	KT-9	5.83E-03
Kgbf	2B78	48.7080	-116.3422	Bonners Ferry	KT-9	9.23E-03
Ksw	85SW01	48.8548	-116.2472	Meadow Creek	KLY-3S	4.66E-02
Kgfc	08RB021	48.7212	-116.4841	Moravia	KLY-3S	1.45E-03
Kgfc	08RB022	48.7205	-116.4780	Moravia	KLY-3S	2.14E-03
Kgfc	08RB021	48.7212	-116.4841	Moravia	KT-9	2.36E-03
Kgfc	08RB022	48.7205	-116.4780	Moravia	KT-9	3.09E-03
Kgd	08RB012	48.6616	-116.4236	Moravia	KT-9	6.10E-04
Ktsp	08RL670	48.6597	-116.4376	Moravia	KT-9	1.30E-02
Ktsp	08RB008	48.6623	-116.4385	Moravia	KT-9	7.55E-03
Ktsp	08RB009	48.6620	-116.4411	Moravia	KT-9	1.06E-02
Kgtc	08RL667	48.5473	-116.3227	Twentymile Creek	KT-9	1.20E-04
Kgtc	08RL668	48.5573	-116.3604	Twentymile Creek	KT-9	2.20E-04
Kgkp	08RL665	48.5149	-116.3205	Twentymile Creek	KT-9	7.80E-03
Kgkp	08RL666	48.5149	-116.3205	Twentymile Creek	KT-9	1.40E-02
Kgkp	08RL669	48.5796	-116.2803	Twentymile Creek	KT-9	2.20E-02
Ymic	86BT00	48.6020	-116.0676	Leonia	KLY-3S	9.65E-04
Ymic	86BT03	48.6188	-116.0698	Leonia	KLY-3S	1.46E-03
Ymic	86BT06*	48.6963	-116.1848	Moyie Springs	KLY-3S	1.50E-03
Ymic	86BT07	48.6917	-116.1839	Moyie Springs	KLY-3S	1.87E-02
Ymi	86BT05**	48.6986	-116.1643	Moyie Springs	KLY-3S	1.00E-03
Ymi	85BT05	48.9183	-116.0573	Canuck Peak	KLY-3S	6.42E-04
Ymi	86BT02**	48.6019	-116.2594	Twentymile Creek	KLY-3S	7.60E-04
Ymi	86BT01	48.6046	-116.2524	Twentymile Creek	KLY-3S	8.47E-04

Belt-Purcell Supergroup

Unit	Sample number	Latitude	Longitude	7.5′ quadrangle	Instrument	Kbulk
Yms_{3-4}	83BT03	48.7955	-116.1352	Meadow Creek	KLY-3S	1.43E-04
Yms_{1-2}	83BT01	48.6431	-116.0568	Curley Creek	KLY-3S	9.16E-05
Yms_{1-2}	83BT02	48.6350	-116.0499	Curley Creek	KLY-3S	1.97E-04
Yms_{1-2}	86MS01	48.5790	-116.0087	Leonia	KLY-3S	9.20E-04
Ysn	84SN01	48.6530	-116.0407	Curley Creek	KLY-3S	2.62E-03
Ysn	86SN01	48.6064	-116.0150	Curley Creek	KLY-3S	2.04E-02
Ysn	85SN03	48.6058	-116.0142	Leonia	KLY-3S	2.96E-04
Ysn	84SN02	48.7510	-116.1178	Line Point	KLY-3S	2.11E-04
Yw	85BT04	48.8035	-116.1197	Line Point	KLY-3S	1.99E-04
Ysr	84SR01	48.7279	-116.0656	Curley Creek	KLY-3S	2.81E-04
Ysr	84SR02	48.7600	-116.0919	Line Point	KLY-3S	2.86E-04
Ysr	85SR03	48.8158	-116.1156	Meadow Creek	KLY-3S	2.50E-04
Yb1	85BT03	48.8498	-116.1141	Line Point	KLY-3S	1.43E-04
Ypt	85BT02	48.8527	-116.1042	Line Point	KLY-3S	1.67E-02
Yph	85BT06	48.9031	-116.1349	Eastport	KLY-3S	2.62E-04
Yph	85BT01	48.8512	-116.1019	Line Point	KLY-3S	3.08E-04
Ypg?	86BT04	48.6769	-116.1241	Curley Creek	KLY-3S	1.35E-04
Ypf	85BT08	48.8896	-116.1119	Canuck Peak	KLY-3S	4.30E-04
Ype	85BT07	48.9038	-116.0785	Canuck Peak	KLY-3S	2.99E-04

* 86BT06 has geochemical affinity with the 1457 Ma (Sears and others, 1998) Paradise sill (Chris Rogers, written commun., 2014).
**86BT02 and 86BT05 have geochemical affinity with the 1469 Ma (Sears and others, 1998) Plains sill (Chris Rogers, written commun., 2014).
KLY-3S is an AGICO spinning susceptometer that was used to measure cylindrical specimens approximately 2.5 cm diameter, 2.2 cm long; KT-9 is a 1995 Kappameter from Exploranium G.S. Ltd. that was used to measure the face of outcrops or multiple sides of hand samples.

Table 1. *Magnetic susceptibilities of some rock units in the Bonners Ferry area.*

Qaf—Alluvial fan deposits (Holocene)—Silt, sand, and pebble to cobble gravel deposited as fans at the mouths of tributary drainages. Unstratified to stratified, unsorted to sorted gravel that consists of subangular to angular clasts derived locally from colluvium and glacial deposits on steep slopes. Thickness 1-10 m (3-33 ft).

Qlm—Lacustrine and fluvial mud deposits (Holocene)—Organic muck, mud, and peat bogs in poorly drained paleoglacial outwash channels, kettles, and ice-scoured bedrock depressions. Interbedded with thin layers of fine sand, silt, and clay. Soils of the Pywell series. Thickness 1-5 m (3-16 ft).

COLLUVIAL AND MASS WASTING DEPOSITS

Qt—Talus (Holocene)—Blocky and tabular, poorly sorted angular clasts of Belt Supergroup, mafic rocks, and granitic rocks that form fans and aprons below cirque headwalls and cliffs oversteepened by glaciation. Includes small protalus ramparts in some cirques. Smaller deposits unmappable at this scale are not separated from bedrock. Generally no soil development. Thickness varies, typically 3-9 m (10-30 ft).

Qc—Colluvial deposits (Holocene)—Blocky and tabular, poorly sorted angular clasts. Generally no soil development. Thickness varies, usually 3-9 m (10-30 ft).

Qls—Landslide deposits (Holocene)—Silt, sand, and gravel in heterogenous deposits of recent and historical landslides.

Qglc—Glaciolacustrine colluvial deposits (Pleistocene to Holocene)—Mixed deposits of silt, sand, and gravel colluvium, slope wash, and small landslides. Steep slopes of reworked and locally transported *Qgl*. Soils are silt loams of the Wishbone-Crash association. Maximum thickness 10 m (33 ft).

Qcg—Colluvial deposits derived from glacial materials (Holocene and Pleistocene)—Silt, sand, and gravel colluvium. Forms debris fans and colluvial aprons along steep valleys and gullies; mostly derived from glacial deposits. Generally in escarpments of *Qglc* where mapped. Includes numerous small unmapped mass movements. Thickness varies, typically 5 m (15 ft).

GLACIAL AND RELATED DEPOSITS

Qgl—Glaciolacustrine deposits (Pleistocene to Holocene)—Massive to well-bedded and finely laminated clay, silt, and sand deposited in Glacial Lake Kootenai at the northward retreating ice margin in the Purcell Trench. Exhibits well-developed rhythmites with scattered dropstones. Contorted bedding and loading structures are common. This unit forms several prominent terrace levels between about 670 and 700 m (2,200 and 2,300 ft) elevation; also forms discontinuous terraces in tributary valleys graded to the Kootenai valley. Mostly well sorted and finely laminated. Overlain by glaciofluvial outwash deposits on terraces and in tributary valleys. Soils are silt loam and silty sandy loams of the Wishbone-Crash association. Exposed thickness as much as 150 m (490 ft).

Qgls—Glaciolacustrine and ice stagnation deposits (Pleistocene)—Fine silt and sand with interbedded bar and channel sand and gravel deposits. Thin laminae to thickly bedded sands with some cross bedding. Irregular topography attributed to eolian dunes, kettle depressions, and deposits of crevasse fills, and (or) eskers. Together, these record a stagnating ice margin (Connors, 1976). Soils are very deep fine sandy loams and loamy sands of the Selle-Elmira association. Thickness ranges from two to tens of meters (6 to >33 ft).

Qg—Glacial deposits, undivided (Pleistocene)—Mostly loose cobbly silty sand with a silty fine sand matrix and pebble-to boulder-sized gravel; includes deposits of till and associated proglacial outwash and glacial sediments. Matrix pale yellow to brown. Clasts dominantly Belt Supergroup, mafic rocks, and granitoid rocks. Scattered large boulders on bedrock and in till. Unstratified to poorly bedded, unsorted to moderately sorted. Present in tributary drainages and on slopes composed of discontinuous remnants of till and kame terraces; on steeper unstable slopes may take the form of mass movements. Locally includes some interbedded lake sediments. Soils mainly silt loam of the Pend Oreille series. Includes *Qgt* and *Qgk*, described below, in map and cross sections where they are not separable at the map scale. Thickness varies from two to 10 m (6 to 33 ft).

Qgo—Outwash deposits, undivided (Holocene and Pleistocene)—Silty and sandy to bouldery gravels. Moderately sorted and rounded pebbles and cobbles. Includes small unmappable deposits of alluvium. Outwash channel deposits in Paradise Valley are remnants of the southward flowing abandoned channel of the Kootenai River and overflow of Glacial Lake Kootenai. Outwash deposits near Moyie Springs are from glaciation of the Moyie River valley. The terraces at the mouth of the Moyie River were graded to Glacial Lake Kootenai. The presence of Glacier Peak Tephra (11,200 B.P.) gives a minimum date for retreat of the ice lobe from the trench (Richmond, 1986). Soils are sandy loams and loamy sands of the Selle-Elmira Association. Thickness as much as 20 m (66 feet).

Qgt—Till deposits (Pleistocene)—Dense silt pebble and cobble till with local boulders deposited by the Purcell Trench lobe of the Cordilleran ice sheet. Poorly stratified compact basal till includes ground moraine and some interbedded proglacial deposits. Deposit includes kame terraces and some outwash along the south margin of the map. Soils include silt loams and gravelly silt loams of the Pend Oreille-rock outcrop and the Stien-Pend Oreille associations. Thickness varies and may exceed 50 m (165 ft).

Qgk—Kame deposits (Pleistocene)—Poorly stratified and compact silty to sandy boulder lodgement till; locally includes ground moraine and some interbedded proglacial and ice contact and outwash deposits. Includes multiple kame terraces along the east side of the Purcell Trench. This unit also probably underlies *Qgl* west and northwest of Bonners Ferry, and records the latest retreat of the Purcell Trench ice lobe. Soils include silt loams and gravelly silt loams of the Stien-Pend Oreille association. Thickness varies and may exceed 50 m (165 ft).

INTRUSIVE ROCKS

Tqm—Quartz monzonite dikes (Eocene)—Fine-grained biotite-hornblende quartz monzonite grading to monzonite. Acicular hornblende 2-5 mm long. Most are spatially associated with lamprophyre dikes at the southern edge of the map; one that crosses the ridge west of Bloom Lake contains abundant subangular to rounded clasts of quartzite and granitic rocks. A single dike is in *Kgc* near its northern extent.

Tl—Lamprophyre dikes (Eocene)—Biotite lamprophyre dikes with 1-2 mm biotite phenocrysts in a fine-grained groundmass. One dike that cuts the Sandpoint conglomerate in the Elmira quadrangle to the south (Lewis and others, 2007b) yielded a 47.15 ± 0.24 Ma $^{40}Ar/^{39}Ar$ date on biotite (Doughty and Price, 2000). This age is in Chron 21n (47.906-46.264 Ma; Cande and Kent, 1995), so dikes of that age should have been magnetized downward. In contrast, a dike one mile northeast of the lower Boulder Creek gaging station is magnetized upward (declination = 148.4, inclination = -71.1, alpha 95 = 9.0), in a reverse field direction (early Eocene direction expected for the location is 167.5, -67.5). Thus, that dike could be slightly older or younger than the one near Elmira. Preservation of this remanent magnetization and the dike's fine grain size and chilled margins indicate that the host rock was cool and likely close to the surface at that time. Elsewhere, dikes are generally deeply weathered and poorly exposed so probably are underrepresented on the map.

TKum—Ultramafic dikes (Eocene or Cretaceous)—Altered massive ultramafic dikes that range in width from one to 30 m (3 to 100 ft) and in grain size from very fine at margins to as coarse as 1 cm in centers. Apparently cut by pegmatites and *Kgf* west of the Purcell Trench, but have chilled margins against fractured quartz and pegmatite veins at southern edge of map. One body immediately south of the map near Bloom Lake contains olivine, actinolite, and chlorite. Cretaceous age based on interpretation that it is intruded by *Kpeg* and *Kgf* south of Cascade Ridge, although some could be younger.

Kgf—Fine-grained granite (Cretaceous)—Equigranular fine-grained biotite granite. Forms small masses on ridge south of Snow Creek and along range front; also present as dikes and small unmapped bodies in other bedrock units west of the Purcell Trench. Age based on similarity to rock in the Colburn quadrangle to the south (Lewis and others, 2007a) dated at 71.8 ± 2.6 Ma (U-Pb on zircons; Richard Gaschnig, written commun., 2014).

Kpeg—Pegmatite (Cretaceous)—Coarse-grained muscovite pegmatite. Bodies typically too small to show at map scale. East of the Purcell Trench in *Kgc* contains dark quartz and open space in irregular, meter-scale intrusions with no sharply defined contacts. West of the Purcell Trench fault, typically as light colored sills or irregular shape bodies distributed approximately along strike of compositional layering and foliation in *Ypmt*. In the southwestern parts of the map, multiple unmapped generations have intruded plutonic rocks as indicated by crosscutting relationships and deformation of the older pegmatites.

Kmg—Muscovite-biotite granite (Cretaceous)—Medium-grained muscovite-biotite granite exposed in a single mass in the southwest corner of map.

Kmlc—Monzonite of Long Canyon (Cretaceous)—Hornblende-pyroxene monzonite to quartz monzonite. Forms elongate body in northeastern part of Priest River complex. Extremely heterogeneous with respect to composition, mafic mineral content, grain size, and texture. Potassium feldspar in 3-8 mm long, crudely tabular grains appears to be mostly microcline, but some could be orthoclase, especially in southern part of body. Average plagioclase is conspicuously unzoned calcic oligoclase. Quartz averages about 3 percent and is rarely greater than 10 percent. Mafic mineral content ranges from 6 to 20 percent, averaging 8 percent. Pyroxene is ferroaugite; hornblende appears to be ferrohastingsite. These mafic constituents are in 3-5 mm grains. Accessory minerals are abundant sphene, allanite, and apatite; locally these minerals are as long as 5 mm. Larger grains are enclosed in groundmass of 1-3 mm equant grains of all minerals. Unit has subtle to pronounced lineation and (or) foliation that varies irregularly on outcrop scale. Contains inclusions of schist and gneiss and is cut by numerous dikes that constitute as much as 20 percent of unit in places. Body highly deformed but where dated near Smith Falls about 9 km (5.5 mi) southwest of Porthill in the northwest corner of the map, is younger (88.8 ± 3.9 Ma, U-Pb on zircons; Richard Gaschnig, written commun., 2014) than adjacent (*Kghc*) megacrystic bodies.

Kgbf—Granodiorite of Bonners Ferry (Cretaceous)—Medium- to coarse-grained biotite granodiorite, with or without muscovite. Local variations include biotite granite and seriate to sparsely porphyritic varieties with salt and pepper diorite(?) inclusions 1-5 cm in diameter. Locally iron stained and altered. Quartz typically strained in 5 mm grains or clusters of 0.5 mm grains and in myrmekitic intergrowths with feldspar. Plagioclase occurs as strongly oscillatory zoned subhedral small grains and aggregates of smaller anhedral grains. Average plagioclase composition is calcic oligoclase. Potassium feldspar is microcline as 1 cm poikilitic anhedral blocks. Biotite, the only mafic mineral, comprises 5-20 percent, averaging 16 percent of rock. This volume is much higher than in most two-mica granitic rocks in region. The biotite occurs as 2-4 mm-thick books. Muscovite is present in enough quantity to be visible in about half of hand specimens; it is typically finer grained than the biotite and commonly bent. Abundant epidote is characteristic; grains in biotite that have euhedral form and allanite cores are probably primary. Sphene as small wedges in some exposures is likely primary; irregular masses with opaque grains (magnetite?) are probably secondary. Other accessories include apatite as prisms shorter than 0.2 mm, magnetite smaller than 0.5 mm, and rare small hornblende inclusions in quartz. Unit has subtle foliation in places and thin, distributed, brittle deformed zones. Some deformed zones in westernmost exposures are heavily chloritized and have calcite in feldspars. Sparse, small, but wide-spread exposures suggest pluton underlies entire valley west of Bonners Ferry. Biotite from a sample collected 4.5 km (2.8 mi) west of Bonners Ferry gave a $^{40}Ar/^{39}Ar$ cooling age of 87.3 ± 0.6 Ma (Doughty and Price, 2000).

Kgv—Granodiorite of Road V-78 (Cretaceous)—Medium- to coarse-grained biotite granodiorite. Found only as isolated exposures in and south of Bonners Ferry; probably underlies large area covered by Quaternary deposits south of Bonners Ferry. Contains abundant 2-3 cm-long microcline megacrysts; almost all are rounded and poorly formed. Plagioclase has strong oscillatory zonation; average composition is sodic andesine. Quartz typically strained in 5 mm grains or clusters of 0.5 mm grains and in myrmekitic intergrowths with feldspar. Biotite is dominant mafic mineral. Most rocks contain hornblende ranging from trace amounts up to 2 percent; it appears to be relict and is best preserved where encased in feldspar. Biotite and hornblende average about 15 percent of rock. Epidote abundant and obvious to unaided eye in all rocks. Sphene is abundant. Rock fabric is lineate and moderately foliate; rounded megacrysts lie in plane of foliation and are elongate parallel to trains of biotite to define lineation. Many sphene crystals are deformed. Some felsic minerals and biotite are tectonically reduced in grain size, but subsequently recrystallized. Interpreted to have conformable contact with *Ypab* and sills in the lower Prichard (Breckenridge and others, 2009). Biotite from a sample collected on the north side of the Kootenai River in Bonners Ferry gave a K-Ar cooling age of 89 Ma (Miller and Engels, 1975), recalculated using current IUGS constants (Steiger and Jaeger, 1977).

Kghc—Monzogranite of Hunt Creek (Cretaceous)—Biotite granodiorite and gneissic granodiorite characterized by 2-10 cm-long potassium feldspar megacrysts where more extensively exposed west of the map. Potassium feldspar is microcline, mostly in megacrysts but also as patches in microperthite. Plagioclase averages oligoclase in composition. Biotite, the sole mafic mineral, comprises 8-14 percent of rock, higher to the north. It commonly occurs as ragged-edged grains or groups of grains, some interleaved with very fine-grained, probably secondary muscovite and opaque mineral(s). Concentration of sphene, the most abundant accessory mineral, mimics concentration of biotite. Allanite very abundant; zircon and apatite are in trace amounts. Unit appears to be early pluton caught up within, and strung out between, other units of Priest River complex (Miller and Burmester, 2004). Zircon U-Pb age between 90 and 95 Ma (Joe L. Wooden, written commun., 1994 in Miller and Burmester, 2004). Archibald and others (1984) reported 94 Ma U-Pb age on zircon from Corn Creek gneiss, which is probable continuation of unit in Canada. A weighted mean U-Pb zircon age of 97.7 ± 3.0 Ma was obtained from a sample of this pluton collected near Smith Falls about 16 km (10 mi) northwest of Copeland, off the northwest corner of the map (Richard Gaschnig, written commun., 2014).

Kbgd—Biotite granodiorite (Cretaceous)—Varied biotite granite to hornblende-biotite granodiorite in isolated poor exposures near the southern boundary that are difficult to relate to other map units. The body east of Kelly Pass is equigranular hornblende-biotite monzogranite with 1-3 mm grains. Biotite about 15 percent, hornblende about 2 percent, epidote about 5 percent, and trace of sphene and magnetite. It has a strong, west-dipping foliation defined in part by inequant biotite clots. The larger body to the east is similar but coarser, megacrystic, and more felsic. It has microcline megacrysts, 5 mm equant quartz and subhedral feldspars, half as much biotite and epidote, and traces of hornblende, sphene, magnetite, and muscovite, the latter probably secondary. It appears to be the northeastern end of swath of sill-like intrusions into *Ypab* that include the Rapid Lighting Creek pluton (Lewis and others, 2007b). Sillimanite found in a rock near the contact suggests that the pressure during intrusions could not have exceeded 6 kb (Redfield, 1986).

Kgc—Granodiorite of Copeland (Cretaceous)—Megacrystic, medium- to coarse-grained hornblende, hornblende-biotite, and biotite granodiorite or monzogranite. Near contact, interlayered with more mafic, equigranular phase. Mafic enclave concentration varies; both cognate inclusions and xenoliths with characteristics of the Prichard Formation are widespread but aligned to form a mappable fabric only near the northern contact. Megacrysts of poikilitic microcline 2-8 cm in length comprise 5-25 percent of the rock. Plagioclase as 4 mm subhedral blocky tablets has strong oscillatory zoning and average composition of calcic oligoclase. Quartz about 25 percent, typically in aggregates 4-8 mm across. Myrmekitic intergrowth of quartz and feldspar common. Biotite in 2-4 mm diameter discrete books is on average twice as abundant as hornblende; together they constitute 10-20 percent of the rock. Accessories include abundant epidote, sphene as 2 mm wedges, and subordinate zircon, apatite, opaque minerals, and allanite. North-south and steep foliation 30 m (100 ft) from nearest *Ksw* appears to parallel contact and crosscut southeast striking fabric in *Ksw*. Cretaceous age based on a weighted mean U-Pb zircon age of 110 ± 2 Ma obtained from a sample collected 17.5 km (11 mi) north of Bonners Ferry (Richard Gaschnig, written commun., 2014). Hornblende and biotite from a sample along the railroad 0.5 km (0.3 mi) southeast of Copeland gave K-Ar cooling ages of 95 Ma and 90 Ma, respectively (Miller and Engels, 1975; recalculated using constants of Steiger and Jaeger, 1977).

Ksw—Syenite of Wall Mountain (Cretaceous)—Medium-gray to blue-gray hornblende quartz syenite. Known only as single small elongate stock in north-central part of map. Highly varied fine- to very coarse-grained, equigranular to porphyritic and hypidiomorphic to idiomorphic granular texture. Accessory epidote (5%), magnetite (3%), and sphene (1%). Foliation is well defined by Carlsbad twinned alkali feldspar, flattened mafic inclusions, and anisotropy of magnetic susceptibility. Foliation parallels contacts with Belt rocks but is truncated by *Kgc* near northwestern limit of unit, where contact is exposed, and to the south, based on its projection south-southeast from westernmost occurrence. Cretaceous age based on U-Pb zircon date of 114 ± 3 Ma on sample collected 19 km (12 mi) north-northeast of Bonners Ferry (Richard Gaschnig, written commun., 2014).

Kgfc—Granodiorite of Falls Creek (Cretaceous)—Chiefly granodiorite, but grading to tonalite in eastern part. Plagioclase averages sodic andesine in composition. Biotite is the lone mafic mineral, averaging 10 percent of the rock. Muscovite is present locally as minor component; probably primary. Accessory minerals include epidote, allanite, apatite, zircon, and opaque minerals. Medium to coarse grained; generally seriate.

Texture and grain size more varied than in tonalite of Snow Peak (*Ktsp*) to east. Unit contains abundant fine- to coarse-grained leucocratic dikes and pods. Composition, texture, and concentration of included leucocratic rocks vary greatly over short distances.

Kgd—Granodiorite (Cretaceous)—Granodiorite exposed locally along the east side of the main body of *Ktsp,* into which it grades. Biotite and locally hornblende bearing. Contains potassium feldspar megacrysts 2-6 cm in length locally deformed into augen, particularly on eastern side of unit. Includes rocks mapped by Miller and Burmester (2004) as tonalite of Snow Peak and by Doughty (1995) as Snow Peak megacrystic granodiorite.

Ktsp—Tonalite of Snow Peak (Cretaceous)—Biotite tonalite, locally ranging to granodiorite. Characterized by abundant pale-green epidote with allanite cores, easily visible in nearly all exposures, and by large, pale, lavender-gray quartz. Average plagioclase composition is intermediate andesine. Typically contains almost no potassium feldspar, but sparse megacrysts are present locally. Quartz commonly elongated into crude, rod-shaped grains as long as 1.5 cm. Biotite is sole mafic mineral in typical *Ktsp*, comprising 11-17 percent of the rock. More mafic and finer grained varieties occur as dikes in southwestern part of map. Porphyritic epidote-bearing hornblende(?)-biotite tonalite dike in *Kgkp* has strong fabric and chilled margins suggesting syntectonic emplacement. Muscovite generally absent, but found sparsely and irregularly in westernmost part of unit; probably secondary. Medium and coarse grained; seriate in much of unit. Subtle to prominent foliation and lineation irregularly developed; generally best developed in eastern part of the main body and the eastern body, which also has more brittle shears. Contains abundant irregularly shaped mafic inclusions ranging from 1 cm to tens of meters. Composition and texture are much more uniform than in most Priest River complex units, but are increasingly varied toward gradational contact with *Kgfc*, around concentrations of mafic inclusions, and near and east of the range front northwest of Round Mountain. There, variation is extreme; some rocks are highly porphyritic and contain hornblende and sphene. These variations in texture and composition are characteristics of the similar-age granodiorite of Kelly Pass and granodiorite of Bonners Ferry, which are not part of Priest River complex. Mixing of intrusions with affinities for both sides of the Purcell Trench is consistent with little displacement across the Purcell Trench fault in this area, or with partitioning of the displacement across several faults. Zircons from ridge south of Snow Creek 9.5 km (6 mi) west-southwest of Bonners Ferry yielded U-Pb age of 116 ± 2 Ma (Richard Gaschnig, written commun., 2014), which is indistinguishable from the ages of *Kgc* and *Kgkp*.

Kgtc—Two-mica monzogranite or granodiorite of Twentymile Creek (Cretaceous)—Medium- to coarse-grained, two-mica monzogranite or granodiorite. Forms single, near-circular pluton centered about 5.5 km (3.4 mi) east of Naples surrounded by granodiorite of Kelly Pass (*Kgkp*) on all but its northwest side. Quartz in aggregates as large as 5 mm in diameter are composed of 1-2 mm, strained grains. Feldspars are similar in size and anhedral to subhedral. Plagioclase is variously zoned and twinned. Average plagioclase composition is calcic oligoclase. Potassium feldspar is microcline with inclusions of quartz, plagioclase, biotite, and near contact with *Kgkp*, hornblende commonly aligned in growth zones. Biotite is the only mafic mineral, comprising 8 percent of the rock. Biotite to muscovite ratio averages 3 to 1. Grain size highly varied. Most of pluton characterized by 5-8 mm wide muscovite as thin books, distinctly larger than other minerals and commonly bent, and as smaller flakes. Accessory minerals include epidote, apatite, zircon, and magnetite, all in grains smaller than 0.5 mm. Sphene, hornblende, and larger magnetite occur in transition to *Kgkp*. Margin is noticeably finer grained than typical interior rocks, but interior contains irregular zones of mixed fine- and coarse-grained rocks. Except for large muscovite grains, texture is even grained to seriate.

Kgkp—Granodiorite of Kelly Pass (Cretaceous)—Highly porphyritic, very coarse-grained biotite-hornblende and hornblende granodiorite and monzogranite. Forms nearly annular ring around *Kgtc*. Quartz occurs as 5 mm masses of 1 mm grains and in myrmekite. Potassium feldspar comprises about 25 percent of rock, mostly as poikilitic blocky microcline megacrysts, 3-10 cm long, but also as anhedral interstitial grains. Plagioclase occurs as 1-5 mm anhedral to subhedral grains, commonly with varied zoning and twinning. Average plagioclase composition is sodic andesine. Mafic mineral content about 16 percent. Hornblende is the sole mafic mineral in some rocks; biotite generally less than but equal to hornblende in others, averages less than 2 percent of rock. Abundant sphene; many grains are 1 mm wedges and likely primary, but anhedral grains with epidote are probably secondary. Most rocks contain 0.5-1.0 percent epidote, probably secondary except for the allanite-cored grains. Zircon, apatite (1-2 mm prisms), magnetite, and allanite are accessory minerals. Includes rock immediately northwest and southeast of *Kgkp* mapped by Miller and Burmester (2004) as *Kgv.* Hornblende from northeastern part of pluton yielded K-Ar (cooling) age of 99 Ma (J. Nakata, written commun., 1993 in Miller and Burmester, 2004). Zircon from south part of pluton 19.5 km (12 mi) south of Bonners Ferry yielded U-Pb age of 116 ± 2 Ma (Richard Gaschnig, written commun., 2014).

Kd—Diorite (Cretaceous)—Coarse-grained epidote-biotite-hornblende diorite. Mapped by Doughty (1995) but not well described. Includes rocks mapped by Miller and Burmester (2004) as granitic and metamorphic rocks, undivided.

Ymi—Mafic intrusive rocks, undivided (Mesoproterozoic)—Fine- to medium-grained, rarer coarse-grained, diorite, diabase, hornblende gabbro, hornblendite, quartz diorite, and biotite granophyre. Typically in sills. Composed of hornblende, biotite, plagioclase, quartz, and opaque minerals (Bishop, 1973; 1976). Hornblende blocky to acicular, plagioclase rarely as centimeter-long laths, quartz as 5 mm blue grains or in granophyre clots as large as 1 cm. Thicker sills are texturally and compositionally zoned; some have fine-grained diabasic borders irregularly grading into coarse gabbro and quartz dioritic granophyre, which is concentrated in upper parts. Variations are common between intrusions and within single bodies both along and across strike. Sills in *Yw* locally greenish where fresh; these contain calcite and possibly actinolite, probably from greenschist facies metamorphism. All within the quadrangle are Moyie sills described by Bishop (1976). Intrusions are generally concordant and tabular but some vary greatly in thickness laterally, include rafts of country rock, branch into multiple sills, end abruptly, or pinch out (Bishop, 1976). Most exposed contacts are sharp, but for some, disruption of adjacent sedimentary rocks indicates that sediments were not lithified at time of intrusion and probably contained interstitial water (Cressman, 1989). Sills lower and higher in the Aldridge Formation (Prichard correlative in Canada) appear to be distinct chemically. The higher set has a higher Ti/Zr ratio than the lower ones (Anderson and Goodfellow, 2000). A more recent regional geochemical study (Rogers and others, 2014a, 2014b) also found at least two distinct geochemical groups. Early intrusions were at shallow levels during or closely following deposition of the lower Aldridge equivalent *Ypab* (Höy and others, 2000; Gorton and others, 2000; Cressman, 1989; Sears and others, 1998; Poage and others, 2000). Generation of *Ypm* was probably synchronous with this activity. Later intrusions have chilled margins and contact aureoles, evidence that they invaded consolidated rock. Age of most sills in and near *Ypab* is probably close to U-Pb dates on zircons near Kimberley, British Columbia (Sullivan Mine, Fig. 1) about 115 km (70 mi) north-northeast of Bonners Ferry (1,468 Ma; Anderson and Davis, 1995) and from southeast of Plains, Montana (Plains sill), about 195 km (120 mi) southeast (1,469 ± 2.5 Ma; Sears and others, 1998). Age of the younger sills may be that of the Paradise sill near the base of the Prichard Formation, also located near Plains (1,457 ± 2 Ma; Sears and others, 1998). Three of six sills in the Prichard Formation sampled in the Bonners Ferry area for geochemistry have affinity with the Plains sill (Chris Rogers, written commun. 2014) so likely belong to the earlier set of Moyie sills. The other three and one sill near the top of *Yw* have affinity with the more highly differentiated Paradise sill suite (Chris Rogers, written commun. 2014) so likely belong to the younger Moyie sill set.

Ymic—Mafic intrusive rocks, Crossport C sill (Mesoproterozoic)—Fine- to coarse-grained hornblende gabbro, quartz diorite, and hornblendite. Finer-grained varieties are typically near bottom and top, but also occur interlayered with coarser phases parallel to upper and lower conformable contacts within the body. Characterized by higher concentration of quartz-rich differentiates, which are more common toward the top, than typical *Ymi*. Granophyre blotches as large as 2 cm common near top in the southern part of the map where the sill is thickest (360 m; 1,200 ft). Hornblendite, locally above that, has acicular amphibole 2 cm long in contrast to common stubby form. Sill is thinner near the north edge of the map (36 m; 120 feet), and where tentatively identified east of the Moyie fault, partly based on occurrence low in *Ype* (30 m; 100 ft). This is the middle or "C" sill of Bishop (1973; 1976) defined east of Crossport near Two Tail Peak. Based on geochemistry of two of the sills sampled (Chris Rogers, written commun. 2014) and differentiation, *Ymic* is probably part of the younger Moyie sill set. The relatively young age of 1,433 Ma from the differentiated top of *Ymic* in *Ype* east of Crossport (Zartman and others, 1982) has been attributed to lead loss during metamorphism (Anderson and Davis, 1995), but additional geochronologic work is needed to evaluate this proposal.

PALEOZOIC ROCKS

€d—Dolomite (Cambrian?)—Light to dark gray dolomite as slightly recrystallized mudstone to wackestone. Some intervals weather dark gray with light spots. Scattered uneven millimeter- to centimeter-scale cryptalgal(?) laminations. Rare grading of indistinct rounded 1-2 mm allochems, and millimeter-scale scours at bases of some allochem-rich layers suggest that the strata face east. Occurs southeast of Meadow Creek as a fault sliver between west-facing, salt-cast-bearing strata of *Yms*$_{3\text{-}4}$, and generally east-facing *Ypf*. Age is based on similarity to the dolomite of Fishtrap Creek 52 km (32 mi) to the south-southeast, also on the east side of the Moyie fault (Harrison and Cressman,1993).

BELT-PURCELL SUPERGROUP

This lithostratigraphic unit spans the international boundary but carries different group, formation, and member names on either side. The groups south of the border are described below, with mention of correlative Purcell Supergroup unit names used north of the Bonners Ferry area. Descriptions of mapped units follow, in young-to-old stratigraphic order.

MISSOULA GROUP

The Missoula Group includes all Belt units above the Piegan Group. It is similar to the Ravalli Group in that it is characterized as a clastic wedge (quartzite, siltite, and argillite) but had a different source (Ross and Villeneuve, 2003). Only the lowest three formations, Mt Shields, Shepard, and Snowslip, are mapped here. Correlatives in Canada of the highest two are the Gateway and Sheppard formations; the lowest is correlated with the Nicol Creek and underlying Van Creek formations.

Mount Shields Formation (Mesoproterozoic)—Red and green quartzite, siltite and argillite, and minor carbonate. Of six members recognized to the south (Burmester and others, 2006), only the bottom four are recognized here; these are combined in pairs due to poor and discontinuous exposure of contacts.

Yms$_{3\text{-}4}$—Mount Shields Formation members 3 and 4 (Mesoproterozoic)—Siltite, argillite, and dolomite. Lower part dominated by green siltite with partings of green and maroon argillite. Polygonal mudcracks, mudchip breccias, and oscillation ripple marks common. Some argillite partings preserve salt crystal casts as square impressions as large as 2 cm, as well as rare hopper crystal casts, especially in maroon rocks. Bedding generally thickens upward, but thin, light green siltite and dark green argillite couplets are scattered throughout. Carbonate rocks and carbonate-bearing rocks, including oolite and boxwork carbonate, are more common toward the top. The boxwork appearance is formed from recessive weathering of dolomite relative to quasi-orthogonal silica veinlets. Dolomite is blue-gray where fresh, and weathers light brown to orange. Thickness calculated from outcrop width in southern end of the swath is 410 m (1,350 ft), but upper contact is the Moyie fault, which cuts down section to the north. Best exposed along east side of the Kootenai River. Corresponds closely to members 3 through 5 of Harrison and others (1992).

Yms$_{1\text{-}2}$—Mount Shields Formation members 1 and 2 (Mesoproterozoic)—Red, pink, green, and gray quartzite, green and red siltite and argillite, and minor carbonate. Green and lighter colors are more common toward base. Quartzite, in 0.3 to rarely 1.0 m beds, is fine grained, mostly flat laminated but also cross laminated, and contains potassium feldspar well in excess of plagioclase. Diffuse, non-resistant brown wisps of carbonate within the quartzite of upper part of unit average a few centimeters in thickness and 10-15 cm in length; some weather recessively to irregular holes. Commonly rippled tops of the quartzite beds have thin red argillite drapes. Siltite and argillite occur as graded and lenticular couplets and microlaminae. Both red and green couplets have dewatering structures, mudcracks, and mudchip breccias. Green strata may have more disrupted zones but red have larger mudchips. Upper approximately 35 m (115 ft) contains several 1-5 dm (rarely 1.0 m) thick layers of purple, buff-weathering, low domal stromatolites as high as 30 cm and as much as 1 m across, with bases of oolite and coarse sand with well-rounded quartz grains. Upper contact placed above highest domal stromatolite zone. Stromatolites well exposed east side of Highway 2 west of the state line. Thickness calculated from outcrop width there about 300 m (1,000 ft). Corresponds closely to members 1 and 2 of Harrison and others (1992).

Shepard Formation (Mesoproterozoic)—Occupies same stratigraphic level as the upper two units of the Wallace Formation mapped to the south (Harrison and Jobin, 1963; Lewis and others, 1999; 2000; 2002). Named Shepard Formation here because it is not markedly different from the Shepard Formation at its type locality and is separated from the carbonate-bearing pinch-and-swell strata typical of the Wallace Formation as found near Wallace, Idaho by carbonate-poor laminated strata (*Ysn*). Subdivision follows Lemoine and Winston (1986) and Burmester (1986).

Ysh_2—Shepard Formation, member 2 (Mesoproterozoic)—Microlaminated to laminated dark gray to black argillite, dark olive-green- to white-weathering siltite, and very fine-grained white quartzite. Laminations are commonly contorted, rarely cracked. Contortions are attributed to soft-sediment deformation. Most siltite and quartzite are in beds about 5 cm thick. Upper contact placed at base of lowest purple argillite or quartzite, or mudcracked siltite and argillite of Yms_{1-2}. Best exposed where unit crosses Kootenai River. Thickness about 120 m (400 ft). Previously also mapped as argillite of Half Moon Lake (Miller and Burmester, 2004).

Ysh_1—Shepard Formation, member 1 (Mesoproterozoic)—Tan- and brown-weathering uneven couplets of green siltite and carbonate-bearing light green argillite. Includes intervals of unevenly laminated dark green siltite and light green argillite, and white quartzite. Some argillite tops are microlaminated. Nonresistant horizontal limestone pods are usually weathered out. Layers of contorted chips, soft-sediment deformation, and centimeter-scale loads and flames are typical. Siltite and quartzite are commonly ripple drift and cross-laminated in beds 2-5 cm thick, or occur as starved ripples in lenticular bedding. Upper contact placed at lowest black argillite of Ysh_2. Best exposures with easy access are in Highway 2 roadcuts west of the state line, sections 29 and 17. Thickness uncertain because of faulting and transposition of bedding where folding intense, but probably less than 500 m (1,500 ft).

Snowslip Formation (Mesoproterozoic)—Divided into three members where mapped to the south as argillite of Howe Mountain (Burmester and others, 2004; 2006); undivided where mapped as lower part of upper Wallace Formation farther south (Lewis and others, 1992; 1999; 2000). Total thickness about 900 m (3,000 ft). Discontinuous exposure and faulting preclude accurate determination of thickness or subdivision for this map.

Ysn—Snowslip Formation (Mesoproterozoic)—Dark green siltite and light green argillite graded and non-graded couplets, green siltite and dark gray argillite couplets, purple siltite and argillite couplets, and green to gray siltite. Lower part is predominately green couplets with a purple zone near its middle. Couplets characteristically have mud and dewatering cracks. Middle part is planar-laminated couplets and microlaminae of greenish-gray- to white-weathering siltite and dark gray to black argillite with millimeter-scale bumps on bedding surfaces, and rusty-weathering 2-8 dm tabular beds of pyritiferous dark gray siltite with black argillite caps. Thinner beds and laminae produce distinct, slaty talus. Similar plane-parallel lamination is widespread in middle of unit elsewhere (Burmester, 1986; Burmester and others, 2006; Lewis and others, 1992; 1999; 2000). Upper part is similar to lower except it lacks purple beds, contains minor carbonate, and perhaps more sulfides. Upper contact placed below concentration of carbonate-bearing lenticular couplets or thick white quartzite of Ysh_1. Most continuous section is southwest of Bonner Lake in northeast corner of section 19. Minimum thickness based on outcrop width is 550 m (1,800 ft).

PIEGAN GROUP

The Piegan Group was resurrected by Winston (2007) to provide group-level continuity across the Belt basin. It includes only the Helena and Wallace formations. Excluded from this redefined Wallace are upper members mapped to the south in the past (e.g., Harrison and Jobin, 1963; Lemoine and Winston, 1986; Lewis and others, 1999; 2000; 2002). Since the carbonate-rich strata below the Wallace in most of Idaho are appreciably different from those in the Helena Formation's new reference section in Glacier National Park, we distinguish these strata as the western facies of the Helena. The correlative unit in Canada to the Piegan Group is the Kitchner Formation.

Yw—Wallace Formation (Mesoproterozoic)—Carbonate-bearing light gray to white siltite and quartzite, and dark gray to black argillite. Some siltite and quartzite are at bases of pinch-and-swell couplets and couples graded to dark argillite tops. Argillite caps characteristically contain ptygmatically folded siltite- or quartzite-filled cracks that taper downward. On bedding plane surfaces, cracks are generally discontinuous and sinuous, occurring isolated but parallel, or as three-pointed stars ("birds foot cracks"), with concave-up argillite between. Less diagnostic components are dark, bluish-gray silty dolomite in beds 1-5 dm thick with molar-tooth calcite ribbons, uneven graded couplets of pale green siltite and calcitic argillite, and white, pyritiferous, very fine-grained calcitic quartzite in 1-5 dm beds, some with hummocky cross stratification. Matrix-supported breccias, with flat clasts 5-20 mm thick and 2-10 cm long in sand and smaller, irregular ones in mud, are near base at east edge of map. Hosts irregular, discontinuous *ZYmi* sills locally at or near top. Upper contact placed above highest black-capped pinch-and-swell couplets. Best exposed northeast of Bonner Lake. Thickness based on map width is 440 m (1,450 ft), less than to the south (790 m, 2,600 ft; Burmester and others, 2004). Zircons from a tuff near upper contact with Snowslip Formation (Winston, 2007) about 170 km (105 mi) east yielded a U-Pb date of 1,454 Ma (Evans and others, 2000).

Yhw—Helena Formation, western facies (Mesoproterozoic)—Pale green carbonate-bearing siltite and argillite. Green siltite and argillite laminae and non-graded couplets at base are commonly disrupted by mudcracks and cm-wide dewatering cracks. Overall, unit is coarser grained than *Ysr*. Dolomite is typically disseminated in tabular beds of tan-weathering greenish siltite and less so in argillite; calcite is concentrated in non-resistant horizontal centimeter-scale pods and vertical ribbons (molar-tooth structure). Carbonate is more common toward top. Decimeter-scale gray limestone beds may have been stromatolites. Contains 1-2 mm pyrite cubes. Includes zones of carbonate-free, laminated to thin-bedded green cross-laminated siltite with lighter green argillite tops and rare graded couplets. Some parting surfaces are rippled; lenticular non-parallel bedding is attributed to ripple and starved ripple lamination. Siliciclastic to carbonate cycles typical of Helena were not recognized, perhaps due to discontinuous exposure. Hosts thin *ZYmi* sill locally. Upper contact, placed at lowest occurrence of black argillite-capped pinch-and-swell couplets, may be too high in places where solution of locally calcitic black caps of *Yw* hinders identification of pinch-and-swell couplets. Best exposed along crest of Haystack Mountain. Thickness about 600 m (2,000 ft). Unit corresponds to the Helena and Empire formations mapped to the east (Harrison and others, 1992).

RAVALLI GROUP

The swath of Ravalli Group strata across the map is only slightly thicker than documented to the southeast (Cressman and Harrison, 1986) and south-southwest (Burmester and others, 2007). Although cosets of thick sets of quartzite used to define the Revett elsewhere (Hayes, 1983; Hayes and Einaudi, 1986) are rarely observed, Revett is mapped on the east side of the Sylvanite anticline (Cressman and Harrison, 1986) and correlated with the middle Creston north of the border where copper-silver-cobalt mineralization is similar to that in the Revett to the south (Hartlaub, 2009). Revett mapped here as the swath of quartzite-rich strata below more typical St. Regis Formation may correspond to the upper Revett mapped elsewhere, and the upper Burke (Yb_2) may correspond to the lower Revett. Correlative unit in Canada, the Creston Formation, includes the uppermost Prichard Formation member mapped here.

Ysr—St. Regis Formation (Mesoproterozoic)—Purple and green siltite, argillite, and quartzite. Lower strata are entirely shades of purple with lighter siltite and darker argillite couplets that are uneven to lenticular and commonly mudcracked. Includes discrete layers of thin mudchips 1-5 cm thick. Green lithologies, more common toward the top, include dark green siltite and lighter green argillite in wavy couplets and couples with rare 1 mm-thick brown dolomitic wisps, pale green tabular very fine-grained quartzite beds (2-5 cm, rarely 10-20 cm) with green argillite caps, and green argillite beds 5-20 cm thick. Dolomite increases upward in millimeter-thick siltite laminae and in pale green siltite layers. Upper contact placed above highest mudcracked and mudchip-bearing purple siltite and argillite; may be placed too low where highest purple obscured. Best exposed in cliffs on northeast side of Haystack Mountain. Minimum thickness 275 m (900 ft).

Yr—Revett Formation (Mesoproterozoic)—White and greenish-gray quartzite, pale purple, gray, and green siltite, and darker gray or purple argillite. Very fine-grained feldspathic quartzite is commonly in 1-5 dm, rarely 1 m, tabular beds that contain parallel, cross, and convolute laminations. Some thicker beds have large trough cross bedding and scoured bases.

Tops are rippled, capped with mudcracked argillite, or missing where beds are amalgamated. Siltite is similar to quartzite and occurs as bases of couplets graded to argillite tops. Mudcracks and chips are distributed throughout. Contains visible magnetite octahedra as reported to the east (Harrison and others, 1992). Poor exposure in area is attributed to fracturing of brittle quartzite into small pieces during deformation. Upper contact placed above highest thick white quartzite. Discontinuously exposed low on the southwest slope of Cross Mountain. Thickness about 450 m (1,500 ft).

Burke Formation (Mesoproterozoic)—Siltite, argillite, and quartzite. Subdivided into two members in this map based on bedding characteristics and sedimentary structures.

Yb_2—Burke Formation, member 2 (Mesoproterozoic)—Green to gray-green siltite, purple and green argillite and siltite, and purple laminated quarzite. Lower part is dominantly 10-20 cm thick siltite beds, typically with macroscopic magnetite octahedra. Slabby partings are commonly along 1-2 mm-thick skins of dark green and some lighter green argillite. Sedimentary features include cross lamination, ball-and-pillow structures, rare convolute lamination, and rare thin mudchips. Purple colors, mudcracks, mudchips, and quartzite increase upward. Quartzite is very fine grained with planar and rarer cross laminae enhanced by purple hematite concentrations. Purple-banded or zebra-striped quartzite in beds 10-30 cm thick occur near top. Upper contact placed at base of lowest thick white quartzite. Best exposed southwest of Cross Mountain. Thickness there approximately 600 m (2,000 ft).

Yb_1—Burke Formation, member 1 (Mesoproterozoic)—Green to gray-green siltite and argillite, and gray to white quartzite. Lower part is dominantly slabby and platy parting 10-20 cm-thick tabular beds of tan- to olive-drab-weathering, greenish-gray siltite, commonly with flat laminations. Magnetite octahedra are as large as 1 mm. Minor carbonate near base occurs as very thin beds and scattered nodules less than 1 cm in length. Light gray, very fine-grained quartzite increases upward, most commonly as bases of undulating couplets and couples that grade up through gray siltite with rare argillite skins. Upper contact placed at lowest occurrence of purple mudcracked argillite and quartzite. Best exposed southwest of Cross Mountain. Thickness there approximately 500 m (1,600 ft).

LOWER BELT SUPERGROUP

The Prichard Formation comprises the lowest strata of the Belt Supergroup. Its equivalent in Canada is the Aldridge Formation. There is probably a continuum in metamorphic grade and deformation between rocks east and west of the Purcell Trench fault. In general, rocks to the east are lower grade and not penetratively deformed whereas those to the west are higher grade and range to extremely recrystallized and penetratively deformed. However, garnets occur in two places east of that fault. One of those is east of the Moyie fault. Sample from *Ypac* near the thrust fault mapped 4.7 km (2.9 mi) southwest of Canuck Peak (see dot on map) yielded a Lu–Hf age of 1,241.3 ± 3.1 Ma (Jeff Vervoort, written commun. 2012). The other is at a similar stratigraphic level near Boulder Mountain west of the "mylonite" fault near the south edge of the map. Garnets also occur locally west of the Purcell Trench fault, but most rocks lack garnet, so garnet growth may be more dependent on chemical composition, alteration, or kinematics of the host rock than pressure and temperature (Pattison and Seitz, 2012). The most recrystallized rocks are found in the southwest. The distinction between metamorphosed Prichard Formation (*Ypmt*) and the gneiss and schist unit (*Ygs*) is thus somewhat arbitrary.

Prichard Formation (Mesoproterozoic)—Dark to light gray siltite, black, gray, and white argillite, gray to white feldspathic quartzite, and white quartzite. Siltite is typically rusty weathering and planar laminated with black or rarely white graded or nongraded argillite tops. Conspicuous bar-code-like patterns in the middle, formed by alternating dark and light siltite, persist regionally (Huebschman, 1973) and have been used as markers for correlation by Cominco exploration geologists (Hamilton and others, 2000). Siltite and argillite couplets, with dark, less commonly light tops, have even and parallel, uneven, wavy, or undulating lamination. Rusty nature of outcrop is due to weathering of abundant sulfides, commonly pyrrhotite. Dominant lamination style and concentration of sulfides vary among members. Quartzite in 2-20 dm beds is light weathering, averages about 60 percent quartz and 20 percent plagioclase, with the remainder mostly white mica and 5 percent biotite (Cressman, 1989). Previous mapping in this area and to the east (Cressman and

Harrison, 1986) subdivided only the top of the Prichard. Here, we apply alphabetic member assignments that Cressman (1989) used south of 48 degrees north latitude. Sedimentary structures recording strong currents or soft sediment deformation, or their absence, are lithologic criteria used to distinguish adjacent members, but assigning quartzite packages with similar characteristics to different members was facilitated by mapping by Cominco with control based on "markers" (Michael Zientek, written commun., 2003). These markers served for the upper units down through *Ype*. Locations of some of these markers (Glombick and others, 2010) aided matching contacts across the international border. Mapping of units below *Ype* is based partly on correlation of the lower-middle Aldridge contact with the top of a concentration of sills just north of the border (Glombick and others, 2010), or the *Ypb-Ypc* contact (Michael Zientek, written commun., 2003) and on the subdivisions of Finch and Baldwin (1984).

Ypt—Prichard Formation, transition member (Mesoproterozoic)—Gray, dark blue-gray, greenish-gray to white siltite, dark gray or black argillite, and white quartzite. Tops of commonly graded, pinch-and-swell siltite and argillite couplets typically have discontinuous cracks that appear spindle-shaped in plan view and ptygma-like in section. Argillite also occurs as 10-50 cm-thick massive beds. Siltite beds 3-10 cm thick are cross laminated or have internal grading from light to dark gray where internal structure is visible; parting more commonly platy than slabby. Brown-weathering carbonate as 1 cm layers and pods are low in the section. Siltite beds increase upward in relative abundance and become olive drab where weathered. Quartzite is fine grained and characterized by dark planar laminations, as well as common ripple and larger low-angle cross lamination, hummocky cross lamination, small "dish" structures, and scattered load structures 5-15 cm in depth. Dark specs within siltite appear to be biotite low in unit but magnetite toward the top. Argillite parting surfaces have 2-5 mm-long rectangular voids where chloritoid(?) weathered out. Upper contact placed above highest recognized pinch-and-swell couplets with dark gray argillite tops, where more even couplets with lighter greenish-gray argillite of *Yb_1* dominates. Best exposed on road to the lookout on south end of Deer Ridge. Thickness 600 m (2,000 ft). Mapped here and immediately to the east (Cressman and Harrison, 1986) as transition zone into overlying Burke Formation whereas elsewhere included in Burke (e.g., Cressman, 1985) or Creston Formation (Brown and others, 1994).

Yph—Prichard Formation, member h (Mesoproterozoic)—Laminated gray siltite and black argillite couplets to microlaminated black argillite with white siltite "lines", and minor brownish siltite and light-weathering quartzite. Laminae and microlaminae are characteristically very even, planar, and continuous. Parting is commonly 2 mm to 5 cm. Weathers with a distinct rusty veneer. Siltite beds are 3-10 cm thick, with slabby parting; quartzite beds are 3-5 dm thick near middle. Includes rare centimeter-scale calcareous silty laminae that weather recessively. Typically forms very platy talus, but where parting is poorly developed, forms bare, rounded outcrops and large boulders. Upper contact placed below lowest occurrence of white quartzite and pinch-and-swell siltite and argillite couplets of overlying *Ypt*. Well exposed across ridge between Keno and Skin Creeks but most accessible on Deer Ridge north of the Lookout. Thickness about 500 m (1,600 ft). Nicknamed the "lined unit" of the Prichard Formation; equivalent to the upper Aldridge Formation in Canada.

Ypg—Prichard Formation, member g (Mesoproterozoic)—Green-gray siltite, dark gray argillite, and gray to white feldspathic quartzite. Siltite beds are even-parallel laminated; some are graded to dark gray argillite. Siltite also occurs as bases of couplets with dark argillite tops. Fine- to very fine-grained quartzite in 1-5 dm, rarely thicker beds decreases upwards from 30-40 percent to 10-20 percent of the strata. Some quartzite beds have dark argillite tops; others have ripple cross lamination and rippled tops, rare argillite clasts 1 by 10 cm with rounded corners, and sole marks. Top placed below thick interval of flat-laminated dark siltite and argillite. Best exposed southwest of Kootenai River northwest of the Homestake Mine. Thickness about 500 m (1,600 ft).

Ypf—Prichard Formation, member f (Mesoproterozoic)—Rusty weathering, dark and light gray siltite, darker gray argillite, and minor lighter quartzite. Siltite is commonly in 1-20 cm tabular, structureless, or even-parallel laminated beds with slabby to platy parting; bases uneven with load-casts, tops are graded to dark argillite; rarely as fine-coarse-fine graded packets, and as light gray bases of couplets graded to darker argillite. Siltite with marker-bed-like layering more common in this unit than others. Quartzite is very fine to fine grained, poorly sorted, biotitic and feldspathic in tabular beds 6-20 cm thick with tops graded to siltite or dark argillite. It comprises 5 to 10 percent of lower part. Bases of some beds are slightly uneven from loading into finer grained material. Where quartzite beds are concentrated in 10-20 m-thick intervals, they form resistant ribs and were mapped separately on some 7.5 minute quadrangles. Ovoid carbonate concretions 30-50 cm in diameter that weather recessively into punky brown masses are common in thicker beds. Upper part is mostly dark siltite with marker-bed-like color layering common, and abundant pyrrhotite locally flattened in bedding planes. Hosts mafic sills "D" and "E" sills of Bishop (1973; 1976) in the south, four or more in the north. Upper contact placed below rippled, cross-laminated and unevenly bedded strata of *Ypg.* Best exposed southwest of Kootenai River between Kafka and John creeks, and east of Moyie River southwest of Spruce Lake. Thickness 1,000-1,300 m (3,300-4,300 ft). Previously subdivided following Finch and Baldwin (1984) into lower member with more quartzite and upper with more argillite (Burmester, 1986); upper part mapped to the east as argillite member of the Prichard Formation (Cressman and Harrison, 1986).

Ypfq—Prichard Formation, member f quartzite (Mesoproterozoic)—Light gray- to white-weathering fine-grained feldspathic quartzite. Mapped only where well enough exposed to show dominance of dm- and m-thick quartzite beds, some in cosets, that range from tabular to broad channel shapes.

Ype—Prichard Formation, member e (Mesoproterozoic)—Light gray- to white-weathering siltite and feldspathic quartzite with darker argillite. Light gray, light-weathering siltite more abundant than darker, rusty-weathering siltite and light gray or light-weathering, very feldspathic fine-grained quartzite. Siltite in 2-10 cm beds dominates over poorly sorted, fine-grained feldspathic quartzite, which varies in concentration from 10 to 40 percent through 10 m of section. Some beds are parallel laminated, but many exhibit features of current traction such as trough cross bedding, ripple and ripple drift cross lamination, rippled tops, and inclusion in quartzite beds of rectangular rip-up clasts 5-15 cm long and white argillite chips, most commonly near bed tops. Soft-sediment deformation and convolute lamination are common; centimeter-scale load casts and ball-and-pillow structures locally abundant; flute and groove casts, channel or loaded bases less common; matrix-supported sedimentary breccia rare. Mud chips litter some bedding surfaces near international border. Carbonate concretions 5 cm to 3 dm appear as dark masses or spots, or brown cavities, but are less common than in *Ypf* and *Ypc*. Some quartzite beds that are coarser grained and less feldspathic than typical of the Prichard contain rounded medium quartz grains, especially concentrated at bed bases, but rounded medium quartz grains are not as prevalent to the east as they are to the west of the Moyie fault. Rounded medium quartz grains also rarely in black argillite near top near northern and southern map boundaries. Carbonate concretions concentrated in some horizons, absent from others. Light-weathering siltite and argillite couplets with uneven to undulating lamination. Thin sill near middle of map east of the Moyie fault has irregular base likely due to intrusion into soft sediment. Some couplets grade up to, or are overlain by, laminated siltite and microlaminated argillite. Quartzite-rich sections commonly have cosets of 2-5, rarely 20 dm-thick beds with little to no argillite between. These form clear ribs and talus slopes. Hosts *Ymic* in lower part. Upper contact placed above highest zone of quartzite with abundant current features and below thick section of uniformly parallel laminated rusty-weathering siltite. Base exposed south side of Leonia Knob, middle well exposed across Border Mountain north of Robinson Lake. Thickness approximately 1,200 m (3,600 ft) including 275 m (900 ft) of *Ymic*) toward the south but 1,000 m (3,400 ft) east of the Moyie fault.

Ypd—Prichard Formation, member d (Mesoproterozoic)—Dark gray siltite, dark gray argillite, and white-weathering gray quartzite. Siltite, and siltite and argillite couplets are predominantly even and parallel laminated to microlaminated and rusty weathering. Less common are 1-3 m-thick intervals of white, very fine- to fine-grained quartzite in rarely amalgamated beds, or rusty-weathering 1-5 dm thick siltite. Exposure generally poor and discontinuous, with quartzite commonly over-represented in float. A zone of contorted beds near end of thin sill, above a larger sill near east edge of map, is atypical. Upper contact placed at lowest occurrence of current-laminated siltite and quartzite below *Ymic.* Thickness uncertain due to poor exposure of contacts 200-500 m (600-1,600 ft).

Ypac—Prichard Formation, members a, b, and c (Mesoproterozoic)—Mapped east of the Moyie fault where base of *Ypc* was not mapped due to discontinuous exposure. Characteristics are mostly of *Ypc* and upper part of *Ypab*, described below.

Ypc—Prichard Formation, member c (Mesoproterozoic)—Dark gray siltite, rusty-weathering, unevenly laminated, dark gray siltite and argillite couplets, and light-weathering quartzite. Fine-grained to rare medium-grained quartzite similar to that of *Ype* but in thinner 3-5 dm-thick beds, is scattered throughout the unit. Some beds have ripple- and cross-lamination, coarser grains at bases and gradation to siltite at the top. Others as thick as 3 m (10 ft) appear structureless or have coarser grains in middle as well as bases. Circular brown spots as large as 6 cm diameter with alteration "halos" probably formed from concentrations of (manganese) carbonate. Hosts one or two undifferentiated sills. Parts are exposed on the northwest side of Dawson Ridge. Top placed above set of quartzite beds and below interval of more evenly laminated, rustier-weathering siltite and argillite. Thickness estimated at 700 m (2,100 ft).

Ypab—Prichard Formation, members a and b (Mesoproterozoic)—Even parallel to undulating, laminated, rusty-weathering, dark gray siltite and argillite couplets, siltite, and lighter quartzite. Couplets typically not graded and less than 1 cm thick; argillite tops locally light weathering. Siltite layers 2-5 cm and 1-5 dm thick and typically dark gray; some that weather light gray are tabular to rarely lenticular with ripple cross lamination. Light gray- to white-weathering quartzite as isolated beds 1-3 dm thick and rarely as 3-10 dm beds amalgamated as thick as 3 m (10 ft) more common toward top; some of these show cross lamination, internal scour and small white mudchips, and load- and flute-cast bases. Intimately associated with a massive unit (*Ypm*) present at or toward the top. Light gray-to white-weathering quartzite as isolated decimeter-scale beds and bases of graded couples, and decimeter- to rare meter-scale beds amalgamated up to several meters thick. Soft-sediment deformation features, including folds and intraformational breccias (conglomerates?) at scales from decimeters to tens of meters are abundant and perhaps characteristic of this unit or at least its upper part near *Ypm*. Hosts Moyie sills that range from tabular to irregular, some with differentiated, quartz- or granophyre-rich tops. Convolute and broken lamination and intraformational conglomerate more common above sills than below. Contact metamorphosed next to *Kgc* with 4-8 mm diameter porphyroblasts (andalusite?). Near south-center part of map, contains small white mica porphyroblasts and sillimanite near *Kbgd*, and becomes increasingly schistose westward. Top placed above horizon of *Ypm* at base of section of relatively abundant meter-thick quartzite that contains medium quartz grains and preserves ripples and cross lamination, or, where such are absent, below a sill at the level where such criteria are found nearby. The base is not exposed, but gravity modeling (Kleinkopf, 1977) suggests that there is a minimum of 3,000 m (10,000 feet) of sedimentary strata between *Ypm* exposed in the Sylvanite anticline (Cressman and Harrison, 1986) and basement. Cross section B-B is consistent with more than 4,000 m (13,000 ft) below *Ypm*, presumed to have been above the section between the Boulder Creek and mylonite faults.

Ypm—Prichard Formation, massive unit (Mesoproterozoic)—Structureless, poorly sorted quartzite and siltite to quartz-rich, fine-grained, biotite granodiorite. Commonly has granofels texture with fine biotite and muscovite. Bedding obscure to absent. Consists largely of plagioclase (in part interstitial), quartz, and biotite; muscovite present as porphyroblasts. Granophyre intergrowths suggest an igneous or magmatic fluid contribution, but rock generally has too much quartz to be entirely igneous (about 44 percent; Redfield, 1986). Locally stratiform but generally discontinuous laterally and non-uniform in thickness. Laminated strata at similar stratigraphic level show soft-sediment deformation more commonly than at other levels in *Ypab*. Commonly floored, less commonly capped, by mafic sills. Locally contains 5-10 percent clasts of laminated siltite and argillite 1-5 cm thick and 3-20 cm long, some of which have apparent reaction rims, others appear deformed. Weathers more rusty than quartzite of *Ype* or *Ypc*. Generally hardest rock of the Prichard Formation, forming rounded exposures and float and large blocky talus. May have formed from increased pore fluid pressure due to heating by the earlier sills (Anderson and Höy, 2000) or from water-rich fluids that had separated from underlying sills (Poage and others, 2000).

METAMORPHIC ROCKS WEST OF THE PURCELL TRENCH FAULT

Yam—Amphibolite (Mesoproterozoic)—Massive, foliated, and lineated amphibolite. Generally fine- to medium-grained hornblende-plagioclase rock, but locally quartzose and (or) garnet-bearing with compositional layering. Presumably the metamorphic equivalent of mafic sills present in the Prichard Formation, with quartzose zones possibly from differentiates.

Ypmt—Metamorphosed Prichard Formation (Mesoproterozoic)—Quartz-biotite-muscovite schist, muscovite-biotite-quartz-plagioclase gneiss and granofels, and muscovite-biotite-plagioclase quartzite. Gneiss and granofels differ mainly in internal fabric development; they occur in layers 1-100 cm thick, but typically 10 cm thick that mimic siltite beds of the Prichard Formation. Schist is commonly 1-5 mm skins between gneiss or granofels layers, less commonly as zones 1-10 dm-thick. Muscovite grains occur both undeformed, typically as grains 1 cm in diameter on schistose partings between compositional layers, and as 2-4 mm grains crenulated in the schistose layers. Locally, schist contains lenses of muscovite 5-20 mm long that may be porphyroblasts or retrograded sillimanite clots. Garnet-bearing only at low elevation from north of Burton Creek to north of Fisher Creek. Small (0.3-0.5 mm) crystals of staurolite were noted in thin section from roadcut 2.4 km (1.5 mi) northwest of Kerr Lake. Compositional layering is mapped in lieu of bedding because metamorphic grade and deformation make transposition of bedding likely, but siltite to argillite graded couplets are still recognizable as fine-grained granofels to schist gradations. Discontinuous exposure and folding preclude deducing facing direction of this unit. Quartzite occurs in 3-8 dm- to rare meter-thick layers. Weak to moderate mylonitic fabric common only locally close to the Purcell Trench. Small bodies of amphibolite, commonly well lineated, less commonly foliated, occur within this unit at least from Cascade Creek to north of Fisher Creek. Commonly intruded by pegmatite and dikes similar to *Kgf*. Also is only host observed for *TKum*. Includes unmapped amphibolite, granitic, and pegmatite bodies, especially toward the west. Considered to be equivalent to the Hauser Lake gneiss (Weis, 1968; Weisenborn and Weis, 1976). Is probably metamorphosed Prichard Formation below *Ypg* if amphibolite is from Moyie sills. Probably not stratigraphically equivalent to exposed *Ypab* because it lacks thick and abundant sills. Most likely *Ypmt* and *Ygs* are stratigraphically lower than observed *Ypab*, and equivalent to unexposed rocks in the core of the Sylvanite anticline (see *Ypab* above). If a west-dipping detachment fault had decapitated the Sylvanite anticline, it might be similar to the east Newport fault with *Ypab* above higher grade rocks of the Priest River complex (Lewis and others, 2008). An alternative is that metasedimentary rocks of the Priest River complex are in a separate, allochthonous thrust plate and differ from the less-metamorphosed Prichard because *Ypmt* and *Ygs* originated in a different part of the Belt basin. This interpretation is consistent with the observation that the 1576 Ma Laclede augen gneiss is fault bounded above apparently autochthonous and below possibly allochthonous Ygs (Lewis and others, 2008) farther southwest.

Ygs—Gneiss and schist (Mesoproterozoic)—Muscovite-biotite-plagioclase-quartz gneiss, and biotite-muscovite and muscovite-biotite schist, both with varied amounts of quartz and plagioclase. Includes unmapped amphibolite, calc-silicate rock, and granitic sills. Mapped only in southwest corner where contiguous with large occurrence to southwest (Lewis and others, 2007a, 2007b; 2008) and as septae in *Ktsp*. Pegmatite bodies more common than in *Ypmt*. Considered to be equivalent to the Hauser Lake gneiss (Weis, 1968; Weisenborn and Weis, 1976). Similar material southwest of Sandpoint has detrital zircon age spectra similar to the Prichard (Doughty and Chamberlain, 2008), so all is probably metamorphosed Prichard Formation. See *Ypmt* above for origin alternatives.

GEOLOGY DISCUSSION

QUATERNARY HISTORY

The Purcell Trench is a major structural and physiographic feature that extends south from Canada over 130 km (80 mi) into the Idaho Panhandle. It is bounded on the east by the Purcell and Cabinet Mountains and on the west by the Selkirk Mountains. The present-day landscape is largely due to glaciation during the last Ice Age. The northern part of the trench is drained by the Kootenai River, which flows west from Montana to Bonners Ferry and then northward into British Columbia. During late Pleistocene glaciation about 15,000 years ago, a lobe of the Cordilleran ice sheet repeatedly advanced southward along the Purcell Trench from Canada (Waitt and Thorson, 1983; Richmond, 1986). Tributary valley glaciers from the Selkirk Range to the west and Purcell Mountains and Cabinet Range to the east contributed to the ice stream. The ice dammed the Kootenai River, formed Glacial Lake Kootenai, and diverted drainage southward through the trench into the Pend Oreille and Spokane River drainages. Thick sections of glacial till, outwash, and lacustrine deposits filled the depression of the Purcell Trench. Cosmogenic ^{10}Be surface exposure ages (mean weighted) constrain the glacial maximum ice limit near the Clark Fork ice dam to the south at 14.1 ± 0.6 ka (Breckenridge and Phillips, 2010). Kame deposits near the United States-Canada border constrain the ice recession (^{10}Be range) from 13.3 to 7.7 ka (William M. Phillips, written commun., 2011). The presence of Glacier Peak tephra (11,200 B.P.) gives a minimum date for retreat of the ice lobe from the trench. After retreat of the Cordilleran ice into British Columbia, the northward drainage of the Kootenai River into the upper Columbia River drainage of Canada was restored. Mountain valley glaciers persisted in the higher cirques in the ranges bordering the Purcell Trench. Holocene alluvium, colluvium, and lacustrine sediments are mostly the product of reworked glacial deposits.

STRUCTURE AND METAMORPHISM

Bedrock in the area probably was deformed during the Mesoproterozoic, possibly the Neoproterozoic, and undoubtedly the Cretaceous and Eocene. To the north in Canada, growth faulting is documented in the upper Belt-Purcell strata (Gardner, 2008), and to the northeast, deformation and metamorphism have been estimated to date from 1350 to 1,320 Ma during the compressive East Kootenay orogeny (Leech, 1962; McMechan and Price, 1982; Pattison and Seitz, 2012). Samples from the Priest River complex to the southwest gave a slightly older age of garnet growth (1,379 ± 8 Ma; Zirakparvar and others, 2010) and a younger age of metamorphism (1,304 ± 32 Ma on zircon rim; Doughty and Chamberlain, 2008). The 1,241.3 ± 3.1 Ma age of garnets (Jeffrey D. Vervoort, written commun., 2013) in *Ypac* is younger yet. This spread of ages suggests that the East Kootenay orogeny was protracted or was multiple events. Younger ages (1,090-1,030 Ma) of titanites in sills near the Sullivan mine suggest Grenville-age metamorphism there (Anderson and Davis, 1995). Later block faulting coincided with deposition of the lower part of the Windermere Supergroup during the Neoproterozoic after about 800 Ma, with deposition of the upper part extending into the early Paleozoic during thermal relaxation (Höy, 1993; Cook and Van der Velden, 1995; Ross and Arnott, 2005). Contraction farther west started in the Jurassic, became the Laramide orogeny about 80 Ma, and culminated to the east about 48 Ma (Madsen and others, 2006). About 80 km (50 mi) southeast of Bonners Ferry, both east- and west-directed thrusting was active around 70 Ma (Fillipone and Yin, 1994). Extension during the Eocene reactivated some thrust faults with normal offset, and activated east-dipping detachment faults that allowed mid-crustal material to extrude to the west out from under upper crustal rocks (Doughty and Price, 2000).

In this map, the Purcell Trench fault and the Moyie fault strike approximately north-south, dividing the map into three domains. The following section addresses from west to east those two faults and deformation in each domain.

WESTERN DOMAIN (PRIEST RIVER COMPLEX)

The main fabrics west of the Purcell Trench are penetrative foliation and lineation in both the metasedimentary rocks and granitic intrusions. Correlative rocks north of the international border experienced at least three phases of deformation: early upright to recumbent open to isoclinal folds, which were refolded along with their axial planar foliations, followed by kinking of schistosity and development of spaced cleavage (Webster and Pattison, 2013). In the Bonners Ferry area, ductile folding as well as more brittle folding and faulting is common in the metasedimentary rocks (*Ypmt*); brittle faulting is found in all units. Most fabrics strike parallel to the Selkirk crest and range front. Mineral lineations in the plutonic rock generally trend northwest with moderate to steep plunges, although exceptions abound. This contrasts with the north-northeast trends of most structural elements north of the border (Webster and Pattison, 2013). Foliated inclusions in igneous bodies and cross-cutting of earlier foliated rocks by less foliated intrusions are consistent with a protracted history of deformation and intrusion, which may help explain the diversity of attitudes. An age of 89 Ma for *Kmlc*, which shares lineation and foliation attitudes with *Yam* at a contact on Russell Ridge, indicates that penetrative deformation continued until at least then.

Easily recognized in the metamorphosed Prichard Formation (*Ypmt*), and perhaps isolated to it, are small asymmetrical folds (S shaped when viewed north), commonly with shallow-dipping axial surface faults. Tops of the folds and dikes cut by the faults are offset to the west, consistent with west-vergent sense of strain inferred from the folds. This deformation may record late-stage west-directed shortening during Cretaceous contraction. Later faulting is manifest near the range front by generally east dipping slickensided surfaces with slickenlines trending east to northeast. Possibly concurrent with this faulting was mylonitization of *Ypmt* quartzite on Cascade Ridge where S-C fabric indicates southeast oblique normal fault motion down to the east. This probably dropped the eastern metasedimentary package against the western block dominated by plutonic rock. Such down-to-the-east faulting may have been coincident with formation of the northern Purcell Trench fault. The low contrast in cooling ages across the eastern contact of *Ypmt* east of Snow Peak compared to the larger contrast across valley fill to the east (Doughty and Price, 2000) indicates that the main trace of the fault is buried in the Kootenai River valley (Purcell Trench).

Deformation west of the Purcell Trench fault was probably protracted or episodic over a long time, and non-uniformly distributed in space. Deformation may have ended by ~70 Ma if the fabric-free felsic dikes in *Ypmt* are related to the non-deformed biotite granite 29 km (18 mi) to the south in the Colburn quadrangle dated as 71.8 ± 2.6 Ma (U-Pb on zircons; Richard Gaschnig, written commun., 2014). L-S fabric in *Kmlc* is shared with *Yam* at their contact over Russell Ridge south of Farnham Peak, suggesting that deformation was concentrated between *Kmlc* and *Ypmt*. However, to the north where *Kmlc* was dated, the eastern contact of *Kmlc* is with less deformed megacrystic *Kghc* (Kphc of Miller and Burmester, 2004), so deformation seems more likely synchronous with intrusion of *Kmlc* than tied to a particular contact. If true, development of fabric and augen in *Kghc* and *Ktsp* is likely older. It is probable that some deformation in *Ypmt* is older yet.

PURCELL TRENCH FAULT

Through most of the area and to the south and north, a sharp metamorphic contrast (amphibolite facies on the west and greenschist-facies on the east; Miller and others, 1999; Pattison and others, 2013) and Eocene cooling ages along the Selkirk Range front (Doughty and Price, 2000), document Eocene uplift west of the Purcell Trench fault. Near the southern map boundary, though, there is a culmination defined by rocks east of the trench having higher metamorphic grade than to the north or south, and an eastward plunging anticline just south of the map (Lewis and others, 2008). Toward this culmination from both north and south, the Purcell Trench fault may split into multiple splays or exist as en echelon segments. The culmination itself may be a segment boundary where tips of northern and southern faults meet, or possibly a large, complex relay ramp. East of where the Purcell Trench fault was shown by Miller and others (1999), there is a lithologic contact that coincides with a modest apparent change in metamorphic grade. Rocks to the west of that contact (*Ypmt*) contain abundant pegmatite bodies, ultramafic dikes, coarse lenses of muscovite, and, on Elmira Peak southwest of Bloom Lake, a garnet assemblage that yielded 6 kb, similar to pressures across the topographic trench (Doughty and Price, 2000). These pressures are higher than the pressure estimate to the east from south of Boulder Mountain (4 kb; Redfield, 1986). The characteristics of *Ypmt* mentioned above are found to the north, west of the Purcell Trench, but not in *Ypab* or higher members of the Prichard Formation to the east. Nor is there the thickness or abundance of amphibolite bodies in *Ypmt* or *Ygs* to match concentration or distribution of Moyie sills in *Ypab* and higher Prichard Formation members. We place the Purcell Trench fault along this lithologic contact.

We see no direct evidence of an earlier low-angle detachment, but there is indirect support from a magnetotelluric (MT) transect across the southern part of the map (Bedrosian and others, 2006; 2007). Interpretation of the MT data traces the Purcell Trench detachment as a moderately conductive zone east from near Naples for 100 km (62 mi), dipping 25 to 30 degrees east down to 20 km (12 mi) depth. Offset of a conductivity contrast interpreted as the Belt/basement contact supports 27 km (17 mi) of Eocene top-to-the-east displacement, which is consistent with seismic reflection interpretation to the north (Varsek and Cook, 1994). Restoration of this structure would place the intrusions currently east of the Purcell Trench fault above those west of it. This reconstruction is attractive because it would allow the existence of a single magmatic belt, but such does not appear possible; there are no plutons known west of the Purcell Trench fault as old as the ones to the east, raising concern about the validity of the MT interpretation.

CENTRAL DOMAIN – STRUCTURES BETWEEN THE PURCELL TRENCH AND THE MOYIE FAULT

Three faults and two intrusive bodies populate the northern part of this domain. The smaller intrusion (*Ksw*) has a distinct planar fabric that appears to be truncated by the larger (*Kgc*) body. Farther south, the structure is more complicated than to the north. Structures are described from north to south and west to east as much as possible.

IRON RANGE FAULT

Named in the Iron Range of British Columbia for a 1 km (0.6 mi) wide zone of east-side-up faults, displacement immediately north of the international border is shown schematically to be 100-200 m (325-650 ft) on individual faults (Brown and others, 1994; Brown and others, 1995). Where the fault is mineralized, about 26 km (16 mi) north of the border, it dips west with west-side-down motion estimated to date from 105 Ma (Galicki and others, 2012). North of Round Prairie, faults between Mission Creek and Mission Mountain may be part of the same system. South of Round Prairie, repetition of the *Ypab-Ypc* contact and kinematic indicators in a broad cataclastic and mylonitic zone are consistent with west-side-down motion on a steep structure, and therefore southward continuation of this system. Displacement across this zone may be larger than on single faults in Canada. The southward extent of the fault is unknown. If it does extend farther south, it would be older than 109 Ma because there is no evidence for it on strike in *Kgc*. This zone is shown on the map as a reverse fault because age of its activity makes it more likely a contractional than an extensional structure. If it predates tilting of the rock it cuts, originally it would have dipped east.

CARROLL CREEK FAULT

Named in British Columbia, it is shown in cross section (Brown and others, 1994) to be steep with east side up and large, possibly 2,500 m (8,200 ft) or more displacement. Repetition of *Ype* across Gillon Creek and a narrow syncline south of Round Prairie are consistent with this sense of motion. It continues southward at least to the *Ksw* contact where it appears to be truncated, and therefore older than 114 Ma. However, it likely continues through *Ypab* and *Ymi* farther south, where it may merge with the Iron Range fault and possibly continue under glacial and lacustrine deposits.

ROUND PRAIRIE FAULT

The postulated northeast-striking fault in Round Prairie is nowhere exposed. Kirkham and Ellis (1926) invoked it to explain lack of continuity of sills across Round Prairie and suggested it was a south-dipping normal fault with vertical throw of more than 300 m (1,000 ft) that truncated faults from the north and continued to the Moyie fault. We show it with north side down because of the apparent left offset of the east-dipping *Ypab-Ypc* contact across it and the lack of *Ype* to the south, and to offset the Iron Range and Carroll Creek faults (presumed to dip east). We also show it offset by the Moyie fault, so it would be intermediate in age between the Iron Range and Moyie faults.

BOULDER CREEK FAULT

The nested intrusive complex of *Kgtc* and *Kgkp* west of the Boulder Creek fault separates two visually distinct sections of the Prichard Formation. To the southwest, northwest-striking, thin-bedded fine siltite and argillite predominate over thin Moyie sills. To the northeast, beyond Prichard strata mostly devoid of sills, the north- to northeast-striking siltite beds are minor in comparison to thick Moyie sills. Some of the difference in strikes may be due to accommodation of the intrusion, but does not account for the change in sill thickness or rock type proportions. The contrast is probably due to fault juxtaposition. However, the line between thick and thin sills appears complexly curved as if distorted by the intrusion. Thus, at least the northern, curved part of the Boulder Creek fault, although shown as a normal fault, may be a contractional structure older than the ~116 Ma intrusions.

Part of the contrast described above is across a south-southeast-striking fault that appears continuous with one along North Callahan Creek south of the map. The fault south of the map has minor offset consistent with displacement down to the southwest. Motion down to the southwest across Boulder Creek is consistent with the highest metamorphic grade rocks in the area being on its northeast side. This sense of motion and its strike parallel to the Hope fault farther south are consistent with an Eocene extensional fault. How or whether it continues to the north is unknown.

East of the Boulder Creek fault is structural domain III of Redfield (1986). Strata in the west have north strikes and homoclinal east dips, but along the ridge between Boulder and Iron mountains dips are east, west, and vertical to rarely overturned. In contrast, cleavage varies little more than 20 degrees from vertical, consistent with axial planar to upright folds with little subsequent deformation. There are also steeply north-plunging stretching lineations of recrystallized quartz and feldspar on foliation surfaces and small folds, which may be sheath folds with axes parallel to the lineations (Redfield, 1986). Locally, the fabric is a foliation with 2-4 mm euhedral garnets that crosscut it, indicating that some penetrative fabric developed before peak metamorphism, possibly in the Mesoproterozoic if garnet age is the same as in *Ypac* east of the Moyie fault.

MYLONITE FAULT

The mylonite fault is so named because there are two zones of unusually deformed sedimentary rock with mylonitic fabrics on strike with each other (Redfield, 1986). The zones are 10-100 m (3 to 30 ft) wide. Non-deformed rocks bracketing the zone are less than 200 m (650 ft) apart. Presumed displacement is up on the west because the garnetiferous rocks are on the west and the east-dipping section which includes *Ypm* on the east is not repeated.

CABOOSE CREEK AND EAST FORK BOULDER CREEK FAULTS

The next major fault to the east of the mylonite fault places locally *Ypm*-bearing *Ypab* on the east against higher strata on the west. Fault relations appear fairly simple along the East Fork of Boulder Creek, but are more complicated to the north where the fault appears to split into two splays. Between the two, west of the gaging station in lower Boulder Creek, there are multiple folds and shear zones, and wide variation in attitudes of both bedding and cleavage. We attribute most deformation to Cretaceous contraction, and show the East Fork of Boulder Creek fault to the north truncated by the Moyie fault. However, an east-dipping breccia and gouge zone in an *Ymi*-vein quartz complex near and north of Boulder Creek may more likely be from Eocene extension. From this fault complex east to the Moyie fault, beds dip moderately to steeply east-northeast with similarly striking but steeper cleavage and foliation and no evidence for refolding. All small asymmetrical folds are S-shaped (viewed north), consistent with west-side-up shear, in contrast to most asymmetrical folds in the other domains that have the opposite sense of rotation.

STAR CREEK FAULT

The Star Creek fault is the farthest east within the domain, but nowhere exposed. It attenuates the upper *Ype* and lower *Ypf* sections against the southward plunging syncline to its east.

MOYIE FAULT

The Moyie fault juxtaposes rocks of the Prichard Formation to the west against younger rocks on the east that range from Mt Shields Formation in the south to Ravalli Group in the north. In the area, it was first described by Kirkham (1939). The west-side-up sense of stratigraphic throw is consistent everywhere. In Canada, the Moyie fault strikes northeast, dips northwest, and Devonian strata in the southeast footwall gives it reverse sense of displacement (Benvenuto and Price, 1979). To the south-southeast of the map, strata on both sides get progressively younger, and the Libby Formation is juxtaposed against Cambrian dolomite. The St. Mary fault, which appears similar in attitude and motion to the Moyie fault north of the border, was intruded by a 94 Ma quartz monzonite stock (U-Pb zircon age; Höy and van der Heyden, 1988), so latest movement on the Moyie fault may be similarly old. To the southeast of the map, latest motion was about 70 Ma (Fillipone and Yin, 1994). However, the Moyie fault may have a long history, including motion during the Neoproterozoic and early Paleozoic (Höy, 1993, McMechan, 1981).

The Moyie fault juxtaposes older rocks on the west (hanging wall) against younger rocks on the east, consistent with it being a thrust, but strata of the hanging and foot walls face each other. This facing direction gives the impression that the fault occupies an attenuated syncline. Support for synclinal fold geometry comes from the slightly east-verging, southward-plunging syncline west of the Moyie fault near the southeast corner of the map, and an open, northward-plunging syncline north of the international border (Brown and others, 1995; Brown, 1998). One hypothesis is that these folds are remnants of a syncline that was paired with the Sylvanite anticline to the east before further contraction was accommodated by faulting. The hypothesis is consistent with the interpretation that the Moyie fault cut down section into the Sylvanite anticline (Harrison and Cressman, 1993) and therefore must be younger. However, locally the Moyie fault and overturned $Yms_{1\text{-}2}$ stromatolites dip steeply east, not the attitude one would expect of a thrust fault. This attitude is most easily explained if the fault and adjacent beds were folded as part of the west limb of the Sylvanite anticline as it continued, or renewed growth after or during thrust faulting. The syncline-thrust system is complicated by an east-side up fault west of the Moyie fault that repeats part of the Prichard section, and numerous faults to the east. It is also complicated by having the sliver of Cambrian(?) dolomite *Cd* on its east side in this map and to the south. Missing is at least the basal Cambrian quartzite common elsewhere (e.g., to the southeast of Sandpoint; Lewis and others, 2008). It is possible that attenuation of the section occurred during contraction but this would require that the Moyie fault (or a splay) cut down section. It seems more likely that the mechanism was down-to-the-west faulting of the eastern footwall of the Moyie fault during Eocene extension. If this faulting were listric, some of the eastward increase in dip of hanging wall strata could date from extension, not earlier contraction.

EASTERN DOMAIN – STRUCTURES EAST OF THE MOYIE FAULT

SYLVANITE ANTICLINE

The major structure east of the Moyie fault is the Sylvanite anticline. Strata in its crest in the northeast corner of the map have low dips; those on its southwest flank dip steeply west. Gravity modeling suggests it is cored by a fault slice of basement (Kleinkopf, 1977). If *ZYmi* cuts folded strata near the hinge, early folding may date from the East Kootenay orogeny (McMechan and Price, 1982). Most faults in the anticline strike north-south with down-to-the-west displacement and likely date from Eocene extension or at least were reactivated at that time. It is possible they could have started as reverse faults, similar to the Iron Range and Carroll Creek faults. Age of the down-to-the-north American Mountain fault across the northern part of the map is unknown, but if it is the continuation of the Round Prairie fault, it would have the same age. Farther south, there are numerous faults that cut out or repeat parts of the section. Some of those mapped as east-vergent thrusts may date from late stages of folding or be coeval with the Moyie fault.

CLEAVAGE-BEDDING RELATIONSHIPS IN CENTRAL AND EASTERN DOMAINS

Attitudes of bedding and cleavage measured at the same outcrops were compiled and analyzed in separate groups on opposite sides of the Moyie fault. Cleavage is best developed in the finest grained rocks where it formed normal to shortening strain. Ideally, folds that form due to shortening develop axial planar cleavage parallel to fold axial surfaces. Based on this relationship, we use the distribution of bedding and cleavage to document some of the region's folding history. Analysis

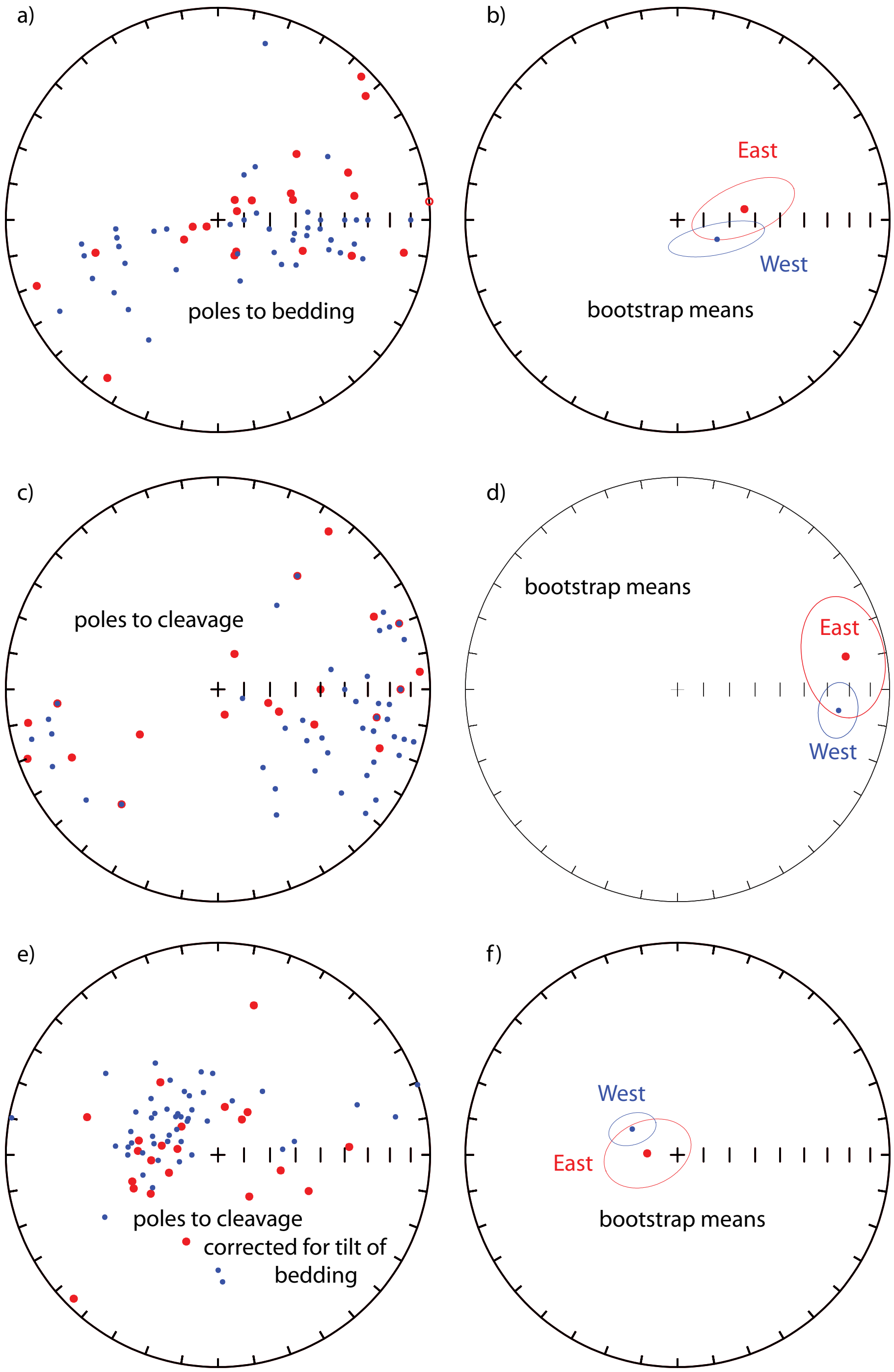

Figure 3. *Equal area plots of poles to bedding and cleavage in the central and eastern domains, west and east of the Moyie fault. (a) Individual bed poles approximate a great circle girdle. (b) Mean directions of poles, with means calculated using a bootstrap method (Tauxe and others, 1991). Ovals include 95 percent of the bootstrap trial results and can be taken as 95 percent confidence limits. (c) and (d) are similar plots but for cleavage measured at the same outcrops. (e) and (f) also are the same but after correction of bedding to horizontal by untilting about strike. Similarity of poles to cleavage in both domains suggest that the rocks were in a common, though not necessary horizontal, frame of reference during cleavage development and that the girdle distributions in (a) and (c) result from later folding of both.*

employed bootstrap methods and programs created for paleomagnetism (Tauxe and others, 1991; Tauxe, 1998) to analyze and plot the results. The simple bootstrap method randomly replaces some of the original dataset with others in the set to build a trial dataset of the same size. The mean and statistics of each trial are calculated for each of 1000 trials. A parametric bootstrap perturbs the replacement data by normal variation consistent with their or the population's statistical parameters.

Figure 3 shows lower hemisphere equal area projections of poles to bed and cleavage surfaces, and their bootstrap means and confidence limits, which include 95 percent of the bootstrap trial means. Observations are shown separately for west of the Moyie fault (central domain) in blue, and east of the fault (eastern domain) in red. Plot (a) shows that individual bed poles form a broad girdle consistent with folding with an axis plunging very gently north-northwest. The bootstrap means (b) are similar for both domains; offset of the means toward the east indicates that more observations came from west-dipping than east-dipping beds in both domains.

Poles to cleavage (c) are more widely distributed, but in general form a girdle similar to that of bedding. Their bootstrap means (d) are shallow and similar in both domains, consistent with cleavage steeper than bedding in both domains. Although ill defined, the girdle distribution suggests at least some of the scatter is due to folding recorded by bed attitudes; therefore, some folding postdates cleavage development. To determine if this was the case, we put cleavage into the bedding frame of reference by rotating bedding, and cleavage along with it, about the local strike by the angle of bed dip. This restores bedding to horizontal. The results for individual cleavage poles (e) and their bootstrap means (f) are at the bottom of Figure 3. Bedding is not shown because all bed poles are now vertical. Poles to cleavage are still scattered, but less so, with the confidence regions shrinking to about 80 and 75 percent of what they were in (d) for west and east of the Moyie fault, respectively. The mean directions are more similar too, separated by about 18 degrees before and 11 degrees after untilting beds and cleavage. More importantly, poles to cleavage are similarly biased to the west in both domains.

If cleavage in rocks on either side of the Moyie fault had formed axial planar to the hypothesized syncline-anticline pair, then cleavage, and therefore poles to cleavage, should be parallel in the post-folding frame of reference, and fan out when the bedding is unfolded. The smaller scatter of cleavage after untilting does not invalidate the hypothesis that folding predated Moyie faulting, only that the observed cleavages were not formed by the folding. What about intensification of folding near the fault where beds face each other? If cleavage had formed axial planar to hinge surfaces of rocks exposed closest to the fault, cleavages in the two domains should have had opposite dips in the current frame of reference, which they do not. Perhaps the correct explanation is the origin of the cleavage in general is unrelated to folding. An alternate explanation is the cleavage formed during regional shear. Similarity of the gently east-dipping cleavage in both domains is consistent with top-to-the-west shear strain in both domains while beds were still horizontal or nearly so. *Ypmt* of the western domain shares this sense of strain. Perhaps the region experienced west-directed thrusting before the better documented eastward episode. If so, then the Purcell Trench detachment could be a reactivated west-directed thrust.

MINERALIZATION

There are several mines and prospects on the map; none were studied for this map. A good resource for information about them is the Idaho Geological Survey web site mines and prospects search (http://www.idahogeology.org/Services/MinesAndMinerals/ Search/), which includes an interactive map. Citations common to most of the larger mines are Kirkham and Ellis (1926), Kiilsgaard (1951), Newton and others (1960), Brackebusch (1969), and Bennett and others (2003).

ACKNOWLEDGMENTS

Fred K. Miller, U.S. Geological Survey, retired, kindly provided field maps, thin sections, and geochemical results from the region that were used extensively in the compilation of the western half of the map. Don Winston shared his views on the Belt Supergroup on numerous occasions and strongly influenced our stratigraphic interpretations. Richard Gaschnig gave dating samples high priority. Permission to access private lands is gratefully acknowledged. Mapping and compilation were supported by the U.S. Geological Survey STATEMAP program and the Idaho Department of Lands.

REFERENCES

Anderson, H.E., and D.W. Davis, 1995, U-Pb geochronology of the Moyie sills, Purcell Supergroup, southeastern British Columbia: Implications for the Mesoproterozoic geological history of the Purcell (Belt) basin: Canadian Journal of Earth Sciences, v. 32, no. 8, p. 1180-1193.

Anderson, H.E., and W.D. Goodfellow, 2000, Geochemistry and isotope chemistry of the Moyie sills: Implications for the early tectonic setting of the Mesoproterozoic Purcell basin, *in* J.W. Lydon, Trygve Höy, J.F. Slack, and M.E. Knapp, eds., The Geological Environment of the Sullivan Deposit, British Columbia: Geological Association of Canada, Mineral Deposits Division, Special Publication No. 1, p. 302-321.

Anderson, H.E., and Trygve Höy, 2000, Fragmental sedimentary rocks of the Aldridge Formation, Purcell Supergroup, British Columbia, *in* J.W. Lydon, Trygve Höy, J.F. Slack, and M.E. Knapp, eds., The Geological Environment of the Sullivan Deposit, British Columbia: Geological Association of Canada, Mineral Deposits Division, Special Publication No. 1, p. 259-271.

Archibald, D.A., T.E. Krogh, R.L. Armstrong, and E. Farrar, 1984, Geochronology and tectonic implications of magmatism and metamorphism, southern Kootenay arc and neighboring regions, southeastern British Columbia, Part II: mid Cretaceous to Eocene: Canadian Journal of Earth Sciences, v. 21, p. 567-583.

Barton, G.J., 2003, Characterization of channel substrate and changes in suspended sediment transport and channel geometry in White Sturgeon spawning habitat in the Kootenai River near Bonners Ferry, Idaho, following the closure of Libby Dam: U.S. Geological Survey Water-Resources Investigations Report 03-4324, 33 p.

Barton, G.J., E.H. Moran, and C. Berenbrock, 2004, Surveying cross sections of the Kootenai River between Libby Dam, Montana, and Kootenay Lake, British Columbia, Canada: U.S. Geological Survey Open-File Report 2004-1045, 42 p.

Bedrosian, P.A., S.E. Box, and Louise Pellerin, 2006, Deep crustal structure between the Selkirk Crest, Idaho and the Whitefish Range, Montana from magnetotelluric imaging: American Geophysical Union, Fall Meeting 2006, abstract S43A-1377.

Bedrosian, P.A., S.E. Box, and Louise Pellerin, 2007, Structure and tectonic evolution of the Belt basin, Montana/Idaho from geophysical constraints: Geological Society of America Abstracts with Programs, v. 39, no. 6, p. 492.

Bennett, E.H., John Kauffman, and V.E. Mitchell, 2003, Site Inspection Report for the Abandoned and Inactive Mines in Idaho on U.S. Forest Service Lands (Region 1), Idaho Panhandle National Forest: Volume VIII: Bonners Ferry Ranger District, Boundary County, Idaho: Idaho Geological Survey Staff Report 03-11, 262 p.

Benvenuto, G.L., and R.A. Price, 1979, Structural evolution of the Hosmer thrust sheet, southeast British Columbia: Bulletin of Canadian Petroleum Geology, v. 27, p. 360-394.

Bishop, D.T., 1973, Petrology and geochemistry of the Purcell sills in Boundary County, Idaho, *in* Belt Symposium, v. 2: Idaho Bureau of Mines and Geology Special Publication, p. 16-66.

Bishop, D.T., 1976, Petrology and geochemistry of the Purcell sills, Boundary County, Idaho and adjacent areas: University of Idaho Ph.D. thesis, 147 p.

Brackebusch, F.W., 1969, Economic geology of the Queen Mountain area, a part of the Purcell Range, Boundary County, Idaho: University of Idaho M.S. thesis, 76 p.

Breckenridge, R.M., and W.M. Phillips, 2010, New cosmogenic ^{10}Be surface exposure ages for the Purcell Trench lobe of the Cordilleran Ice Sheet in Idaho: Geologic Society of America Abstracts with Programs, v. 42, no. 5, p. 309.

Breckenridge, R.M., R.F. Burmester, M.D. McFaddan, and R.S. Lewis, 2009, Geologic Map of the Bonners Ferry Quadrangle, Boundary County, Idaho: Idaho Geological Survey Digital Web Map 108, scale 1:24,000.

Breckenridge, R.M., R.F. Burmester, and R.S. Lewis, 2010, Geologic Map of the Ritz quadrangle, Boundary County, Idaho, by R.M. Breckenridge, R.F. Burmester, and R.S. Lewis: Idaho Geological Survey Digital Web Map 119, scale 1:24,000.

Breckenridge, R.M., R.F. Burmester, R.S. Lewis, and M.D. McFaddan, 2011, Geologic map of the Copeland quadrangle, Boundary County, Idaho: Idaho Geological Survey Digital Web Map 139, scale 1:24,000.

Breckenridge, R.M., R.F. Burmester, R.S. Lewis, M.D. McFaddan, and J.D. Lonn, 2012, Geologic Map of the Curley Creek quadrangle, Boundary County, Idaho, and Lincoln County, Montana: Idaho Geological Survey Digital Web Map 148, scale 1:24,000.

Breckenridge, R.M., R.S. Lewis, R.F. Burmester, and M.D. McFaddan, 2013, Geologic Map of the Farnham Peak quadrangle, Boundary County, Idaho: Idaho Geological Survey Digital Web Map 158, scale 1:24,000.

Brown, D.A., 1998, Geological compilation of the Yahk (east half) and Yahk River (west half) map areas, southeastern British Columbia: British Columbia Ministry of Energy and Mines, Minerals Division, Geological Survey Branch, Geoscience Map 1998-2, scale 1:50,000.

Brown, D.A., J.A. Bradford, D.M. Melville, A.S. Legun, and D. Anderson, 1994, Geology and mineral deposits of Purcell Supergroup in Yahk map area, southeastern British Columbia (82F/1), *in* B. Grant and J.M. Newell, eds., Geological fieldwork 1993: a summary of field activities and current research Geological Fieldwork 1993: British Columbia Ministry of Energy, Mines and Petroleum Resources Paper 1994-1, p. 129-151.

Brown, D.A., J.A. Bradford, D.M. Melville, and P. Stinson, 1995, Geology of the Yahk map area, southeastern British Columbia (82F/1): British Columbia Ministry of Energy, Mines and Petroleum Geological Survey Branch Open File 1995-14, scale 1:50,000.

Burmester, R.F., 1985, Preliminary geologic map of the Eastport area, Idaho and Montana: U.S. Geological Survey Open-File Report 85-517, 10 p., scale 1:48,000.

Burmester, R.F., 1986, Preliminary geologic map of the Leonia area, Idaho and Montana: U.S. Geological Survey Open-File Report 86-554, 13 p., scale 1:48,000.

Burmester, R.F., R.M. Breckenridge, R.S. Lewis, and M.D. McFaddan, 2004, Geologic map of the Clark Fork quadrangle, Bonner County, Idaho: Idaho Geological Survey Digital Web Map 25, scale 1:24,000.

Burmester, R.F., R.M. Breckenridge, M.D. McFaddan, and R.S. Lewis, 2006, Geologic map of the Derr Point quadrangle, Bonner and Shoshone counties, Idaho: Idaho Geological Survey Digital Web Map 59, scale 1:24,000.

Burmester, R.F., R.S. Lewis, M.D. McFaddan, R.M. Breckenridge, D.M. Miller, and F.K. Miller, 2007, Geologic map of the Cocolalla quadrangle, Bonner County, Idaho: Idaho Geological Survey Digital Web Map 91, scale 1:24,000.

Burmester, R.F., R.M. Breckenridge, R.S. Lewis, and M.D. McFaddan, 2009, Geologic Map of the Moravia quadrangle, Boundary County, Idaho: Idaho Geological Survey Digital Web Map 107, scale 1:24,000.

Burmester, R.F., R.M. Breckenridge, M.D. McFaddan, and R.S. Lewis, 2010a, Geologic Map of the Meadow Creek quadrangle, Boundary County, Idaho: Idaho Geological Survey Digital Web Map 120, scale 1:24,000.

Burmester, R.F., R.M. Breckenridge, M.D. McFaddan, and R.S. Lewis, 2010b, Geologic Map of the Moyie Springs quadrangle, Boundary County, Idaho: Idaho Geological Survey Digital Web Map 118, scale 1:24,000.

Burmester, R.F., R.M. Breckenridge, R.S. Lewis, and M.D. McFaddan, 2011a, Geologic map of the Eastport quadrangle, Boundary County, Idaho: Idaho Geological Survey Digital Web Map 140, scale 1:24,000.

Burmester, R.F., R.M. Breckenridge, R.S. Lewis, and M.D. McFaddan, 2011b, Geologic map of the Hall Mountain quadrangle, Boundary County, Idaho: Idaho Geological Survey Digital Web Map 138, scale 1:24,000.

Burmester, R.F., R.M. Breckenridge, M.D. McFaddan, R.S. Lewis, and J.D. Lonn, 2012a, Geologic Map of the Canuck Peak quadrangle, Boundary County, Idaho, and Lincoln County, Montana: Idaho Geological Survey Digital Web Map 151, scale 1:24,000.

Burmester, R.F., M.D. McFaddan, R.M. Breckenridge, R.S. Lewis, and J.D. Lonn, 2012b, Geologic Map of the Leonia quadrangle, Bonner and Boundary counties, Idaho, and Lincoln County, Montana: Idaho Geological Survey Digital Web Map 149, scale 1:24,000.

Burmester, R.F., R.M. Breckenridge, M.D. McFaddan, R.S. Lewis, and J.D. Lonn, 2012c, Geologic Map of the Line Point quadrangle, Boundary County, Idaho, and Lincoln County, Montana: Idaho Geological Survey Digital Web Map 150, scale 1:24,000.

Cande, S.C., and D.V. Kent, 1995, Revised calibration of the geomagnetic polarity timescale for the Late Cretaceous and Cenozoic: Journal of Geophysical Research, v. 100, p. 6093-6095.

Chugg, J.C., and M.A. Fosberg, 1980, Soil survey of Boundary County, Idaho: United States Department of Agriculture Soil Conservation Service and United States Department of the Interior Bureau of Indian Affairs in cooperation with University of Idaho, College of Agriculture, Idaho Agricultural Experiment Station, 75 p.

Connors, J.A., 1976, Quaternary history of northern Idaho and adjacent areas: University of Idaho, Ph. D. thesis, 504 p.

Cook, F.A., and A. Van der Velden, 1995, Three-dimensional crustal structure of the Purcell anticlinorium in the Cordillera of southwestern Canada: Geological Society of America Bulletin, v. 107, p. 642-664.

Cressman, E.R., 1985, The Prichard Formation of the lower part of the Belt Supergroup, Proterozoic Y, near Plains, Sanders County, Montana: U.S. Geological Survey Bulletin 1553, 64 p.

Cressman, E.R., 1989, Reconnaissance stratigraphy of the Prichard Formation (Middle Proterozoic) and the early development of the Belt basin, Washington, Idaho, and Montana: U.S. Geological Survey Professional Paper 1490, 80 p.

Cressman, E.R., and J.E. Harrison, 1986, Geologic map of the Yaak River area, Lincoln County, northwest Montana: U.S. Geological Survey Miscellaneous Field Studies Map MF-1881, scale 1:48:000.

Doblas, Miguel, 1998, Slickenside kinematic indicators: Tectonophysics, v. 295, p. 187–197.

Doughty, P.T., 1995, Tectonic evolution of the Priest River complex and the age of basement gneisses: Constraints from geochronology and metamorphic thermobarometry: Queen's University Ph.D. thesis, 408 p.

Doughty, P.T., and K.R. Chamberlain, 2008, Protolith age and timing of Precambrian magmatic and metamorphic events in the Priest River complex, northern Rockies: Canadian Journal of Earth Sciences, v. 45, no. 1, p. 99-116.

Doughty, P.T., and R.A. Price, 2000, Geology of the Purcell Trench rift valley and Sandpoint conglomerate: Eocene en echelon normal faulting and synrift sedimentation along the eastern flank of the Priest River metamorphic complex, northern Idaho: Geological Society of America Bulletin, v. 112, no. 9, p. 1356-1374.

Evans, K.V., J.N. Aleinikoff, J.D. Obradovich, and C.M. Fanning, 2000, SHRIMP U-Pb geochronology of volcanic rocks, Belt Supergroup, western Montana: evidence for rapid deposition of sedimentary strata: Canadian Journal of Earth Sciences, v. 37, no. 9, p. 1287-1300.

Fillipone, J.A., and An Yin, 1994, Age and regional tectonic implications of Late Cretaceous thrusting and Eocene extension, Cabinet Mountains, northwest Montana and northern Idaho: Geological Society of America Bulletin, v. 106, no. 8, p. 1017-1032.

Finch, J.C., and D.O. Baldwin, 1984, Stratigraphy of the Prichard Formation, Belt Supergroup: *in* S.W. Hobbs, ed., The Belt, Abstracts with Summaries, Belt Symposium II, 1983: Montana Bureau of Mines and Geology Special Publication 90, p. 5-7.

Galicki, M., D. Marshall, R. Staples, D. Thorkelson, C. Downie, C. Gallagher, R. Enkin, and W. Davis, 2012, Iron oxide ± Cu ± Au deposits in the Iron Range, Purcell Basin, Southeastern British Columbia: Economic Geology, v. 107, p. 1293–1301.

Gardner, D.W., 2008, Sedimentology, stratigraphy, and provenance of the upper Purcell Supergroup, southeastern British Columbia, Canada: implications for syn-depositional tectonism, basin models, and paleogeographic reconstructions: University of Victoria, BC, M.S. thesis, 76p, http://hdl.handle.net/1828/911

Glombick, P., D.A. Brown, and R.F. MacLeod (compilers), 2010, Geology, Yahk, British Columbia: Geological Survey of Canada, Open File 6153, scale 1:50,000.

Gorton, M.P., E.S. Schandl, and Trygve Höy, 2000, Mineralogy and geochemistry of the Middle Proterozoic Moyie sills in southeastern British Columbia: *in* J.W. Lydon, Trygve Höy, J.F. Slack, and M.E. Knapp, eds., The Geological Environment of the Sullivan Deposit, British Columbia: Geological Association of Canada, Mineral Deposits Division, Special Publication No. 1, p. 322-335.

Hamilton, J.M., R.G. McEachern, and O.E. Owens, 2000, A history of geological investigations at the Sullivan deposit, *in* J.W. Lydon, Trygve Höy, J.F. Slack, and M.E. Knapp, eds., The Geological Environment of the Sullivan Deposit, British Columbia: Geological Association of Canada, Mineral Deposits Division, Special Publication No. 1, p. 4-11.

Harrison, J.E., and E.R. Cressman, 1993, Geology of the Libby thrust belt of northwestern Montana and its implications to regional tectonics: U.S. Geological Survey Professional Paper 1524, 42 p.

Harrison, J.E., and D.A. Jobin, 1963, Geology of the Clark Fork quadrangle, Idaho-Montana: U.S. Geological Survey Bulletin 1141-K, p. 1-38.

Harrison, J.E., E.R. Cressman, and J.W. Whipple, 1992, Geologic and structural maps of the Kalispell 1° x 2° quadrangle, Montana, and Alberta and British Columbia: U.S. Geological Survey Miscellaneous Investigations Series Map I-2267, scale 1:250,000.

Hartlaub, R.P., 2009, Sediment-hosted stratabound copper-silver-cobalt potential of the Creston Formation, Purcell Supergroup, southeastern British Columbia (parts of NTS 082G/03, /04, /05, /06, /12), *in* Geoscience BC Summary of Activities 2008, Geoscience BC, Report 2009-1, p. 123–132.

Hayes, T.S., 1983, Geologic studies on the genesis of the Spar Lake strata-bound copper-silver deposit, Lincoln County, Montana: Stanford University Ph.D. dissertation, 340 p.

Hayes, T.S., and M.T. Einaudi, 1986, Genesis of the Spar Lake strata-bound copper-silver deposit, Montana: Part I, Controls inherited from sedimentation and preore diagenesis: Economic Geology, v. 81, p. 1899-1931.

Höy, Trygve, 1993, Geology of the Purcell Supergroup in the Fernie west-half map area, southeastern British Columbia: British Columbia Ministry of Energy, Mines and Petroleum Resources Bulletin 84, 157 p.

Höy, Trygve, and P. van der Heyden, 1988, Geochemistry, geochronology, and tectonic implications of two quartz monzonite intrusions, Purcell Mountains, southeastern British Columbia: Canadian Journal of Earth Sciences, v. 25, no. 1, p. 106-115.

Höy, Trygve, D. Anderson, R.J.W. Turner, and C.H.B. Leitch, 2000, Tectonic, magmatic and metallogenic history of the early synrift phase of the Purcell basin, southeastern British Columbia, *in* J.W. Lydon, Trygve Höy, J.F. Slack, and M.E. Knapp, eds., The Geological Environment of the Sullivan Deposit, British Columbia: Geological Association of Canada, Mineral Deposits Division, Special Publication No. 1, p. 33-60.

Huebschman, R.P., 1973, Correlation of fine carbonaceous bands across a Precambrian stagnant basin: Journal of Sedimentary Petrology, v. 43, p. 688-699.

Kiilsgaard, T.H., 1951, Descriptions of some ore deposits and their relationships to the Purcell sills, Boundary County, Idaho: Idaho Bureau of Mines and Geology Pamphlet 85, 31 p.

Kirkham, V.R.D., 1939, The Moyie-Lenia overthrust fault: Journal of Geology, v. 38, no. 4, p. 364-374.

Kirkham, V.R.D., and E.W. Ellis, 1926, Geology and ore deposits of Boundary County, Idaho: Idaho Bureau of Mines and Geology Bulletin 10, 78 p.

Kleinkopf, M.D., 1977, Geophysical interpretations of the Libby thrust belt, northwestern Montana: U.S. Geological Survey Professional Paper 1546, 22 p.

Lane, E.W., 1947, Report of the subcommittee on sediment terminology: Transactions of the American Geophysical Union, v. 28, no. 6, p. 936-938.

Leech, G.B., 1962, Metamorphism and granitic intrusions of Precambrian age in southeastern British Columbia: Geological Survey of Canada Paper 62–13, 8 p.

Lemoine, S.R., and Don Winston, 1986, Correlation of the Snowslip and Shepard formations of the Cabinet Mountains with upper Wallace rocks of the Coeur d'Alene Mountains, western Montana, *in* S.M. Roberts, ed., Belt Supergroup: A Guide to Proterozoic Rocks of Western Montana and Adjacent Areas: Montana Bureau of Mines and Geology Special Publication 94, p. 161-168.

Lewis, R.S., R.F. Burmester, M.D. McFaddan, B.A. Eversmeyer, C.A. Wallace, and E.H. Bennett, 1992, Geologic map of the upper North Fork of the Clearwater River drainage, northern Idaho: Idaho Geological Survey Geologic Map 20, scale 1:100,000.

Lewis, R.S., R.F. Burmester, M.D. McFaddan, P.D. Derkey, and J.R. Oblad, 1999, Digital geologic map of the Wallace 1:100,000 quadrangle, Idaho: U.S. Geological Survey Open-File Report 99-390, scale 1:100,000.

Lewis, R.S, R.F. Burmester, J.D. Kauffman, and T.P. Frost, 2000, Geologic map of the St. Maries 30 x 60 minute quadrangle, Idaho: Idaho Geological Survey Geologic Map 28, scale 1:100,000.

Lewis, R.S., R.F. Burmester, R.M. Breckenridge, M.D. McFaddan, and J.D. Kauffman, 2002, Geologic map of the Coeur d'Alene 30 x 60 minute quadrangle, Idaho: Idaho Geological Survey Geologic Map 33, scale 1:100,000.

Lewis, R.S., S.E. Box, R.M. Breckenridge, R.F. Burmester, and M.D. McFaddan, 2007a, Geologic map of the Colburn quadrangle, Bonner County, Idaho: Idaho Geological Survey Digital Web Map 89, scale 1:24,000.

Lewis, R.S., R.F. Burmester, and R.M. Breckenridge, 2007b, Geologic map of the Elmira quadrangle, Bonner County, Idaho: Idaho Geological Survey Digital Web Map 90, scale 1:24,000.

Lewis, R.S., R.F. Burmester, R.M. Breckenridge, M.D. McFaddan, and W.M. Phillips, 2008, Preliminary geologic map of the Sandpoint 30 x 60 minute quadrangle, Idaho and Montana, and the Idaho part of the Chewelah 30 x 60 minute quadrangle: Idaho Geological Survey Digital Web Map 94, scale 1:100,000.

Madsen, J.K., D.J. Thorkelson, R.M. Friedman, and D.D. Marshall, 2006, Cenozoic to Recent configurations in the Pacific Basin: Ridge subduction and slab window magmatism in western North America: Geosphere, v. 2, p. 11–34.

McFaddan, M.D., R.F. Burmester, R.M. Breckenridge, and R.S. Lewis, 2009, Geologic Map of the Naples quadrangle, Boundary and Bonner counties, Idaho: Idaho Geological Survey Digital Web Map 109, scale 1:24,000.

McKee, E.D., and G.W. Weir, 1963, Terminology for stratification and cross-stratification in sedimentary rocks: Geological Society of America Bulletin, v. 64, p. 381-390.

McMechan, M.E., 1981, The Middle Proterozoic Purcell Supergroup in the southwestern Purcell Mountains, British Columbia, and the initiation of the Cordilleran miogeocline, southern Canada and adjacent United States: Bulletin of Canadian Petroleum Geology, v. 29, p. 583-641.

McMechan, M.E., and R.A. Price, 1982, Superimposed low-grade metamorphism in the Mount Fisher area, southeastern British Columbia: Implications for the East Kootenay orogeny: Canadian Journal of Earth Sciences, v. 19, p. 476-489.

Miller, D.A., Jr., 1973, Geology of the Leonia Knob area, Boundary County, Idaho: University of Idaho M.S. thesis, 103 p.

Miller, F.K., and R.F. Burmester, 2004, Geologic map of the Bonners Ferry 30' x 60' quadrangle, Idaho and Montana: U.S. Geological Survey Miscellaneous Field Studies Map MF-2426, scale 1:100,000.

Miller, F.K., R.F. Burmester, R.E. Powell, D.M. Miller, and P.D. Derkey, 1999, Digital geologic map of the Sandpoint 1° x 2° quadrangle, Washington, Idaho, and Montana: U.S. Geological Survey Open-File Report 99-0144, scale 1:250,000.

Miller, F.K., and J.C. Engels, 1975, Distribution and trends of discordant ages of the plutonic rocks of northeastern Washington and northern Idaho: Geological Society of America Bulletin, v. 86, p. 517-528.

Newton, Joseph, Denis LeMoine, C.N. Adams, A.L. Anderson, and J.A. Shively, 1960, Study of two Idaho thorite deposits: Idaho Bureau of Mines and Geology Pamphlet 122, 53 p.

Pattison, D.R.M., and J.D. Seitz, 2012, Stabilization of garnet in metamorphosed altered turbidites near the St. Eugene lead–zinc deposit, southeastern British Columbia: Equilibrium and kinetic controls: Lithos, v. 134-135, p. 221-235.

Pattison, D.R.M., D.P. Moynihan, and C.R.M. McFarlane, 2013, *Revised and updated 2nd edition*. Field guide to metamorphism and tectonics in the Rocky Mountains, Purcell anticlinorium and Kootenay Arc, southern Alberta and British Columbia (Calgary-Radium-Cranbrook-Kimberley-Creston-Riondel-Nelson-Salmo): Geological Association of Canada field guide series, GeoCanada 2010 meeting, Calgary, Alberta, 153 p.

Petit, J.P., 1987, Criteria for the sense of movement on fault surfaces in brittle rocks: Journal of Structural Geology, v. 9, p. 597-608.

Poage, M.A., D.W. Hyndman, and J.W. Sears, 2000, Petrology, geochemistry, and diabase-granophyre relations of a thick basaltic sill emplaced into wet sediments, western Montana: Canadian Journal of Earth Sciences, v. 37, no. 8, p. 1109–1119.

Redfield, T.F., 1986, Structural geology of part of the Leonia quadrangle in northeast Idaho: Western Washington University M.S. thesis, 156 p.

Richmond, G.M., 1986, Tentative correlation of deposits of the Cordilleran ice-sheet in the northern Rocky Mountains, *in* V. Sibrava, D.Q. Bowen, and G.M. Richmond, eds., Quaternary Glaciations in the Northern Hemisphere: Quaternary Science Reviews, v. 5, p. 129-144.

Rogers, C., A. J. Mackinder, R.E. Ernst, and B. Cousens, 2014a, Geochemical and geochronological characterization of multiple generations of mafic magmatism in the Belt-Purcell and Wyoming basins, focusing on the Moyie-Purcell ca. 1460 ma intraplate magmatic event: Geological Society of America Abstracts with Programs, v. 46, no. 5, p. 70.

Rogers, C., A.J. Mackinder, R.E. Ernst, and B. Cousens, 2014b, Sm-Nd isotopic, and geochemical characterization of mafic magmatism in the Belt-Purcell and Wyoming basins, comparing the single pulse ca. 780 Ma Gunbarrel and the multiple pulses of the Moyie-Purcell ca. 1460 Ma intraplate magmatic events: Geological Society of America Abstracts with Programs, v. 46, no. 6, p.708.

Ross, G.M., and R.W. Arnott, 2005, Regional geology of the Windermere Supergroup, southern Canadian Cordillera and stratigraphic setting of the Castle Creek study area, *in* T.H. Nilsen, R.D. Shew, G.S. Steffens, and J.R.J. Studlick, eds., Atlas of Deep-Water Outcrops: AAPG Studies in Geology 56, p. 1-16.

Ross, G.M., and M. Villeneuve, 2003, Provenance of the Mesoproterozoic (1.45 Ga) Belt basin (western North America): another piece in the pre-Rodinia paleogeographic puzzle: Geological Society of America Bulletin, v. 115, p. 1191-1217.

Sears, J.W., K.R. Chamberlain, and S.N. Buckley, 1998, Structural and U-Pb geochronological evidence for 1.47 Ga rifting in the Belt basin, western Montana: Canadian Journal of Earth Sciences, v. 35, p. 467-475.

Simpson, C., and S.M. Schmid, 1983, An evaluation of criteria to deduce the sense of movement in sheared rocks: Geological Society of America Bulletin, v. 94, p.1281-1288.

Staatz, M. H., 1972, Thorium-rich veins of Hall Mountain in northernmost Idaho: Economic Geology, v. 67, no. 2, p. 240-248.

Steiger, R.H., and E. Jaeger, 1977, Subcommission on geochronology—Convention on the use of decay constants in geo- and cosmochronology: Earth and Planetary Science Letters, v. 36, no. 3, p. 359-362.

Streckeisen, A.L., 1976, To each plutonic rock its proper name: Earth-Science Reviews, v. 12, p. 1-33.

Tauxe, L., 1998, Paleomagnetic Principles and Practice: Dordrecht, The Netherlands, Kluwer Academic Publishers, 299 p.

Tauxe, L., N. Kylstra, and C. Constable, 1991, Bootstrap statistics for paleomagnetic data: Journal of Geophysical Research, v. 96, p. 11,723-11,740.

Varsek, J.L., and F.A. Cook, 1994, Three-dimensional crustal structure of the eastern Cordillera, southwestern Canada and northwestern United States: Geological Society of America Bulletin, v. 106, p. 803-823.

Waitt, R.B. Jr., and R.M. Thorson, 1983, The Cordilleran ice sheet in Washington, Idaho, and Montana, *in* S.C. Porter, ed., Late Quaternary Environments of the United States, v. 1, The Late Pleistocene, p. 53-70.

Webster, E.R., and D.R.M. Pattison, 2013, Metamorphism and structure of the southern Kootenay Arc and Purcell Anticlinorium, south-eastern British Columbia (parts of NTS 082F/02, /03, /06, /07): Geoscience BC Summary of Activities 2012, Geoscience BC, Report 2013-1, p. 103–118.

Weis, P.L., 1968, Geologic map of the Greenacres quadrangle, Washington and Idaho: U.S. Geological Survey Geologic Quadrangle Map GQ-734, scale 1:62,500.

Weisel, C.J., 2005, Soil Survey of Boundary County, Idaho: United States Department of Agriculture, Natural Resources Soil Conservation Service in cooperation with United States Department of the Interior, Bureau of Land Management, University of Idaho College of Agriculture; and Idaho Soil Conservation Commission, Idaho Agricultural Experiment Station, Part I, 144 p.

Weisenborn, A.E., and P.L Weis, 1976, Geologic map of the Mount Spokane quadrangle, Spokane County, Washington, and Kootenai and Bonner counties, Idaho: U.S. Geological Survey Geologic Quadrangle Map GQ-1336, scale 1:62,500.

Winston, Don, 1986, Sedimentology of the Ravalli Group, middle Belt carbonate, and Missoula Group, Middle Proterozoic Belt Supergroup, Montana, Idaho and Washington, *in* S.M. Roberts, ed., Belt Supergroup: A Guide to Proterozoic Rocks of Western Montana and Adjacent Areas: Montana Bureau of Mines and Geology Special Publication 94, p. 85-124.

Winston, Don, 2007, Revised stratigraphy and depositional history of the Helena and Wallace formations, mid-Proterozoic Piegan Group, Belt Supergroup, Montana and Idaho, *in* P.K. Link and R.S. Lewis, eds., Proterozoic Geology of Western North America and Siberia: SEPM (Society for Sedimentary Geology) Special Publication No. 86, p. 65-100.

Zartman, R.E., Z.E. Peterman, J.D. Obradovich, M.D. Gallego, and D.T. Bishop, 1982, Age of the Crossport C sill near Eastport, Idaho, *in* R.R. Reed and G.A. Williams, eds., Society of Economic Geologists' Coeur d'Alene Field Conference: Idaho Bureau of Mines and Geology Bulletin 24, p. 61-69.

Zirakparvar, N.A., J.D. Vervoort, W. McClelland, and R.S. Lewis, 2010, Insights into the metamorphic evolution of the Belt-Purcell basin; evidence from Lu-Hf garnet geochronology: Canadian Journal of Earth Sciences, v. 47, Issue 2, p. 161.